Novel functional crystalline polymers with dynamic bonds

（動的結合で高分子量化した結晶性高分子の新規機能）

Nobuhiro Oya　　大矢　延弘

Department of Chemistry and Biotechnology

School of Engineering, The University of Tokyo

Chapter 1. General Introduction

Chapter 2. Photoinduced mendable network polymer from poly(butylene adipate) end-functionalized with cinnamoyl groups

Chapter 3. Crystalline polymers with a self-mending ability at room temperature

Chapter 1. General Introduction

1-1 Materials based on crystalline polymers

Polymer materials are widely used and important in industry areas because of their low cost (for example expensive equipments are not necessary for fabrication), low density compared with other materials, and so on. In addition to these factors, polymer materials have excellent advantages. Their properties are easy to be controlled, which fulfills the requests of specific applications. Indeed, there are various kinds of polymer materials from glassy hard thermosets to soft elastomers. Their Properties and functions depend on their chemical structures (such as kinds of monomer, polymer structures, and composition of block polymers) and their morphologies. Controlling these factors is important for fabrication of desired polymer materials.

Crystalline polymers having crystals dispersed in amorphous matrix have attracted continual interest as a significant kind of polymeric materials. The hard crystalline phase gives hardness and the soft amorphous phase gives toughness to materials, hence they become tougher than amorphous polymers.[1] For regulating properties and functions of crystalline polymers, crystallinity[2], crystalline structure[3] and crystal orientation[4] provide important factors, adding to the above-mentioned factors.

For example, many crystalline polymers were studied about improvement of mechanical and thermal properties by annealing.[5] Annealing induces activation of internal mobility of polymer chains and following reorganization of crystalline and amorphous regions. These result in increase of crystallinity, improved order and thickening of crystalline and amorphous lamellae, hence obtaining materials with superior properties[2,6].

On the other hand, spherulites and shish kebabs are two dominant morphologies in crystalline polymer. While spherulites isotropically grow in quiescent condition from

melt, melt flowing during crystallization or melt drawing enhances crystallization and induces shish kebab which consists of central extended chains (shish) and folded chain lamellae grown from center.[7] Though the mechanism of shish kebab formation is still under question, films with shish kebab structures have excellent properties. For instance, polyethylene is well-known and widely applied crystalline polymer for such as pipes for water, gas and oil, food packaging, and so on. Melt drawn films of ultrahigh molecular weight polyethylene with shish kebab structures exhibit excellent mechanical properties i.e. tensile moduli $\geq$ 58 GPa and strength $\geq$ 0.95 GPa at room temperature.[8]

As described above, properties of crystalline polymer materials are attributed to crystals and some simple processes affect them. Therefore, crystallization is an important factor for crystalline polymer materials and controlling it is necessary for fabricating materials which fulfill orders for applications.

1-2 Dynamic bonds

Dynamic bonds, whose formation and dissociation can be repeatedly controlled, are very attractive and researched in various areas.[9] Dynamic bonds include reversible covalent bonds i.e. “dynamic covalent bond”, and noncovalent interactions.

Noncovalent interactions, for instance hydrogen bonds[10] and metal-ligand coordination bonds[11] (Figure 1-2-1), connect molecules without covalent bonds and allow molecules self-assembly. These are under equibrium condition.

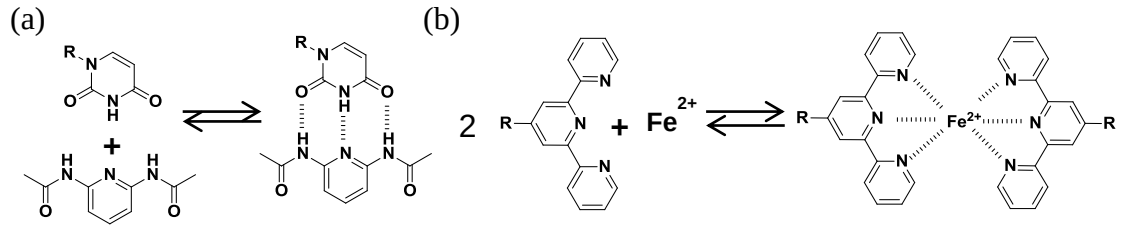

Figure 1-2-1. Noncovalent interactions:(a) hydrogen bond, (b) metal-ligand coordination bonds

On the other hand, dynamic covalent bonds, such as disulfide bonds[12] and acylhydrazone[13] (Figure 1-2-2), form covalent bonds and breaking occurs by external stimuli. Therefore, these are more stable than noncovalent interactions.

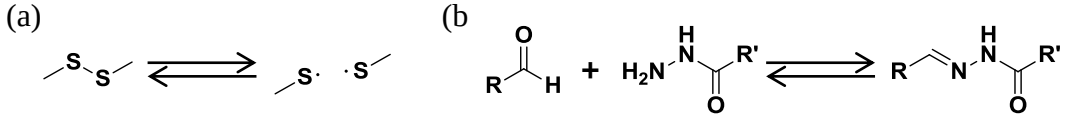

Figure 1-2-2. Dynamic covalent bonds(a) disulfide bonds, (b) acylhydrazone

These dynamic bonds are utilized for material construction. Materials whose components are connected by dynamic bonds are able to respond to external stimuli by virtue of reversible formation and breaking of dynamic bond. These natures give materials characteristic functions.[14] For example, thermo- and chemo- responsive metallo-supramolecular polymer were reported.[15] 4-Oxy-2,6-bis-(10-methylbenzimidazolyl)pyridine (Mebip) ditopic endcapped poly(tetrahydrofuran) with various ratios of $Zn^{2+}$and Eu^{3+} became thermoplastic elastomers. Increasing of the Eu^{3+} ratio resulted in a change in fluorescence of the films from blue to red, which came from the emission from the Eu^{3+} : Mebip complexes. The

fluorescence of the films was sensitive to heating or addition of triethyl phosphate and changes from red to blue due to displacement of Eu^{3+} from Mebip ligands.

Materials consisting of dynamic bonds exhibit their functions with breaking or formation of dynamic bonds. Each dynamic bond has a specific stimulus for breaking or formation such as heating, light, pH and mechanical force. Hence properties, functions and responsiveness of materials depend on constituent dynamic bonds[1]. In summary, materials with dynamic bonds have stimuli responsive properties, and breaking or/and formation of bonds are one of the most important factors for exhibition of their functions.

1-3 Crystalline polymers with dynamic bonds

There are many studies about crystalline polymers with dynamic bonds.[16] Materials consisting of crystalline polymer with dynamic bonds have attractive functions such as mechanochromic responses[17], recyclability [18], and so on. For instance, Prof. Yoshie and coworkers researched about crosslinked crystalline polymers by Diels-Alder (DA) reactions. DA reactions such as furan and maleimide forms dynamic bonds. (Figure 1-3-1)

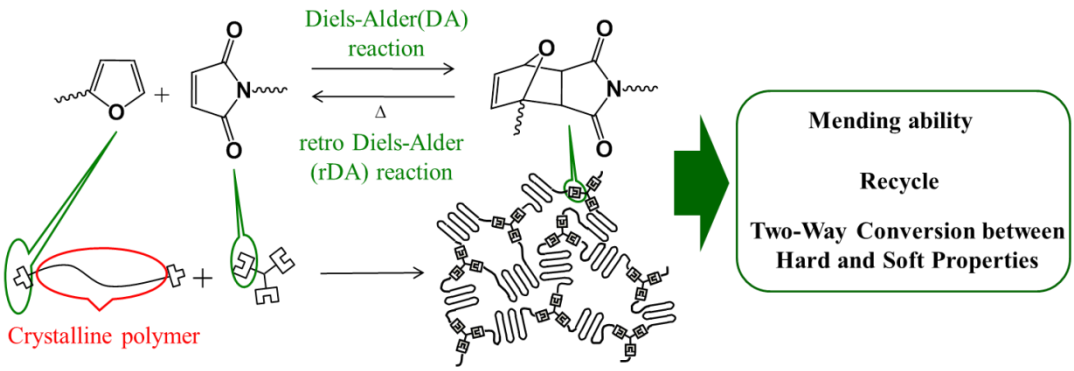

Figure1-3-1. Crystalline polymers cross-linked by Diels-Alder reaction.

The cycloaddition via DA reactions of furan and maleimide progresses at mild temperature without byproducts while dissociation to form furan and maleimide (retro-DA[rDA] reaction) occurs above 100 ^{o}C. Network polymers formed form telechelic polymers having two furan moieties as end groups and linkers having three maleimide moieties via DA reactions have characteristic properties such as mendability[19], recyclability[20] and two way conversion between hard and soft properties[21]. These are obtained from reversible bonding formation of dynamic bonds. Mendability and recyclability issued from breaking of DA adducts by cracking to form furan and maleimide and re-formation of DA adducts. Additionally, preferential progress of crystallization or crossliking gave different materials with different mechanical properties.[21]

Like these research, dynamic bonds can functionalize crystalline polymers. Additionally, properties and functions of materials depend on kinds of dynamic bonds and crystalline polymers.

1-4 Purpose of this study

In this research, the author obtained novel functional materials from crystalline polymers with dynamic bonds by controlling dynamic bonds and crystallization. As described in Chapter1-1, various factors of crystalline polymers such as monomer, polymer structures, and composition of block polymers can be controlled. Especially, crystallization is one of the most important and controllable factors. Crystallinity, crystalline structure, crystal orientation and morphologies usually become candidate for controllable factors to obtain desired materials. In addition, crystallization rate is also controllable. Crystallization rate means the rate of crystallization from molten

conditions to the equibrium crystallinity. Crystallization rate can be controlled by temperature Crystallization rate becomes slower at higher temperature and polymers do not crystallize above melting temperature. Modification of bulky units or closslinking also makes the crystallization rate slow.

As described in Chapter 1-2, materials consisting of dynamic bonds can exercise their functions with formation or breaking of dynamic bonds. In this study, the author fabricates novel functional materials consisting of crystalline polymers and dynamic bonds by controlling above described two factors, i.e., crystallization rate and formation of dynamic bonds. Their control has never been done in the previous research of crystalline polymers with dynamic bonds and this result in regulating materials' higher order structure and molecular mobility, leading to new functions. By controlling them, two treatments become possible. One is dynamic bond formation induced by crystallization control. Controlling rate of crystallization from melt states can maintain high molecular mobility. This makes dynamic bonds possible to form, resulting in exhibition of materials' functions or fabrication of functional materials. Another is competitive progress of crystallization and dynamic bond formation by controlling temperature. In previous research of crystalline polymers with dynamic bonds, crystallization or formation of dynamic bonds preferentially proceeded and rate of crystallization was not under control.[16,18,21] Their control has possibility to give different materials with different mechanical properties from those previously reported.

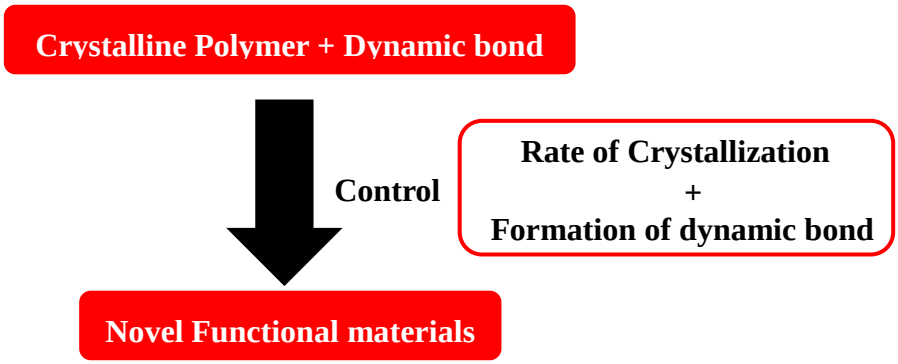

Figure1-4-1. Novel functional materials obtained from crystalline polymers with dynamic bonds by controlling crystallization and formation of dynamic bond

There are three topics in this study about fabrication of functional materials.

First topic is about a photoinduced mendable network polymer. Heating and photoirradiation in material preparation gave a cross-linked polymer by dynamic bonds. These dynamic bonds were preferentially broken by damage and recovered by re-photo irradiation and heating to mend.

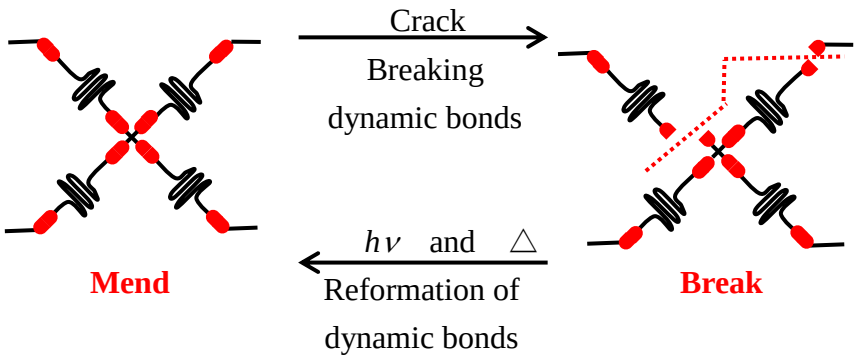

Figure1-4-2. Schematic view of first topic

Second topic is about crystalline polymers with mending ability at room temperature. Dynamic bonds in polymer architectures were broken by cutting materials. Controlling

rate of crystallization by end-functionalization of prepolymer enabled breaking of dynamic bonds to re-form between cut surfaces. This re-formation of dynamic bonds resulted in mend at room temperature.

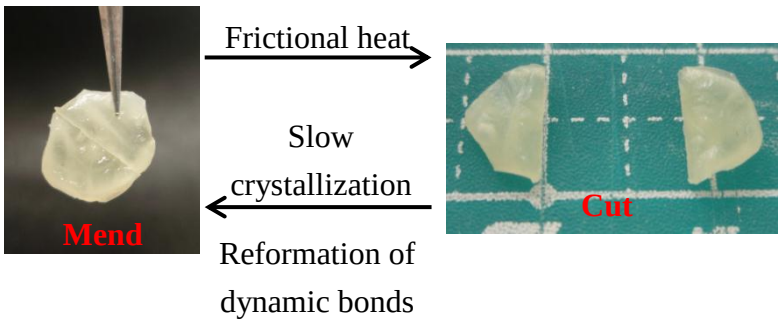

Figure1-4-3. Schematic view of second topic

Third topic is about mechanical property tuning of semicrystalline network polymers by controlling rates of crystallization and crosslinking. When semicrystalline crosslinked network polymer by DA adducts, controlling rates of crystallization and crosslinking by temperature made mechanical properties adaptable. Especially, their concurrent progress resulted in tough materials.

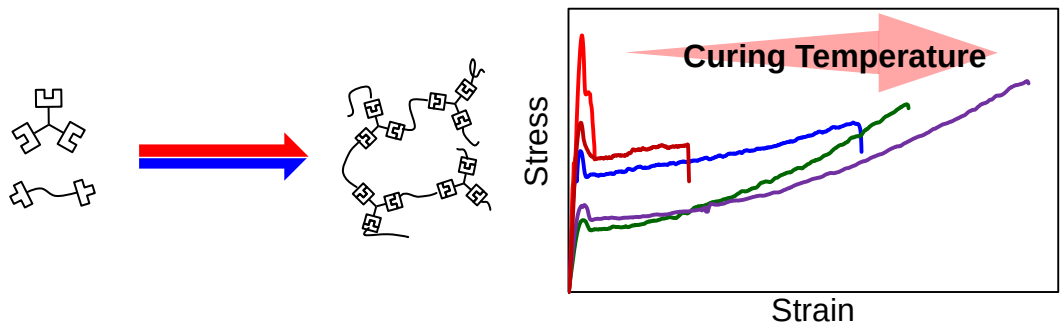

Figure1-4-3. Schematic view of third topic

1-5. References

[1](a)Y. Men, G.J. Strobi, Macromol. Sci. Phys. **2001**. *B40*, 775, (b) Y. F. Men, J. Strol, *Phys. Rev. Lett*. **2003**, *91*, 095502

[2]S. Humbert, O. Lame, G. Vigier, *Polymer*, **2009**, *50*, 3755.

[3]Y. Wada, *Elecrtonic Properties of Polymers*, J. Wiley & Sons, New York, 1982.

[4]Y. Li, K. Shen, *Polym. Int.*, **2009**, *58*, 484.

[5] (a)D. A. Blackadder, P. A. Lewell, *Polymer*, **1970**, *11*, 147, (b) H. W. Bai, Y, Wang, Z. J. Zhang, L. Han, Y. L. Li, L. Liu, Z.W. Zhou, Y. F. Mwn, *Macromolecules*, **2009**, *42*, 6647, (c)S. B. Xie, S. M. Zhang, H. J. Liu, G. M. Chen, M. Feng, H. L. Qin, F. S. Wang, M. S. Yang, *Polymer*, **2005**, *46*, 5417.

[6] S. Song, J. Feng, P, Wu, *J. Polym. Sci. Part B: Polym. Phys.* **2011**, *49*, 1347.

[7](a)M. J. Hill, A. Keller, *J. Macromol. Sci*. **2005**, *181*, 75, (b)Z. Jiang, Y. Tang, J. Rieger, H. F. Enderle, D. Lilge, S. V. Roth, R. Gehrke, Z. Wu, Z. Li, X. Li, Y. Men, *Europ. Polym. J.*, **2010**, 1866, (c)J. A. Odell, D. T. A. Grubb, A. Keller, *Polymer*, **1978**, *19*,617.

[8] M. Nakae, H. Uehara, T. Kanamoto, *Macromolecules*, **2000**, *33*, 2632.

[9] R. J. Wojtecki1, M. A. Meador, S. J. Rowan, *Nature materials*, **2011,** *10*, 14.

[10] (a)F. H. Beijer, R. P. Sijbesma, J. A. J. M. Vekemans, E. W. Meijer, H. Kooijman and A. L. Spek, J. Org. Chem., **1996**, *61*, 6371, (b) A. J. Wilson, *Soft Matter*, **2007**, *3*, 409.

[11] U. Mansfeld, M. D. Hager, R. Hoogenboom, C. Ott, A. Winterb, U. S. Schubert, *Chem. Commun*. **2009**, 3386.

[12] H. Otsuka, S. Nagano, Y. Kobashi, T. Maeda, A. Takahara, *Chem. Commun.* **2010**, 1150.

[13] J. F. F. Andersen, J. M. Lehn, *J. Am. Chem. Soc.* **2011**, *133*, *10966.*

[14] (a) D. A. Davis, A. Hamilton, J. Yang, L. D. Cremar, D. V. Gough, S. L. Potisek, M. T. Ong, P. V. Braun, T. J. Martínez, S. R. White, J. S. Moore, N. R. Sottos, *Nature* **2009**,*459***,** 68, (b) A. M. Kushner, J. D. Vossler, G. A. Williams,Z. A. Guan, *J. Am. Chem. Soc.***2009**, *131*, 8766.

[15] J. R. Kumpfer, J. Jin, S. J. Rowan, *J. Mater. Chem.* **2010**, *20***,** 145.

[16](a) B. K. Kim, S. Y. Leea, J. S. Lee, S. H. Baek, Y. J. Choi, J. O. Lee, M. Xu, *Polymer*, **1998**, *39*,2803, (b) M. Fan, Z. Yu, H. Luo, S. Zhang, B Li, *Macromol. Rapid Commun.* **2009**, *30*, 897, (c) P. Y. W. Dankersa, E. N.M. van Leeuwena, G. M. L. van Gemertb, A. J. H. Spieringa, M. C. Harmsenc, L. A. Brouwerc, H. M. Janssenb, A. W. Bosmand, M. J. A. van Luync, E.W. Meijera, *Biomaterials*, **2006**, *27*, 5490.

[17] G. O. Brayn, B. M. Wong, J. R. Mcelhanon, *Appl. Mater. Interfaces*, **2010,** *2*, 1594.

[18] T. Defize, R. Riva, J. M. Raquez, P. Dubois, C. Jerome, M. Alexandre, *Macromol. Rapid Commun*., **2011**, *32*, 1264.

[19] N. Yoshie, M. Watanabe, H. Araki, K. Ishida, *Polym. Degrad. Stab*.**, 2010,** *95*, 826.

[20] M. Watanabe, N. Yoshie, *Polymer*, **2006**, *47*, 4946.

[21] K. Ishida, N. Yoshie, *Macromolecules*, **2008**, *41*, 4753.

Chapter 2.

Photoinduced mendable network polymer from poly(butylene adipate) end-functionalized with cinnamoyl groups

Introduction

Mendable materials which are capable of repairing cracks either automatically or by applying heat- and photo-activation have attracted great interest in recent years.[1]

Figure 2-1 Mendable materials

They can maintain their original mechanical properties for a longer period. Mending ability of polymers has been achieved by mixing microencapsules containing repairing agents into polymer matrices[2] and by introducing dynamic bonds such as dinamic covalent bonds,[2-5] supramolecular self-assemblies[6-8] and functional moieties which generate a reactive group by bond cleavage[9] to polymer chains.

On the other hand, a number of publications have reported on reversible photoinduced network polymers based on dimerization of photoreactive groups such as benzylidenephthalimidines[6], coumarines[11], anthracene[12] and cinnamate[13]. Although various applications including photolithography[12] and fabrication of liquid crystals[14] have been examined until now, only a few reports are on photoinduced mendable materials using photodimerization[15,16]. Chung et al.[15] developed a photo-mendable polymer by using cinnamate dimer. A double network polymer was synthesized by simultaneous progress of photoinduced radical polymerization of methacrylate monomers and photo-dimerization of cinnamoyl groups in

1,1,1-tris-(cinnamoyloxymethyl) ethane (TCE). Cracks on this polymer were repaired by irradiation of λ>280 nm, which promoted the recovery of TCE-based network structure. Froimwicz et al.[16] presented a photo-mendable hyperbranched polymer based on anthracene dimers. The surface scratches of this polymer could be mended by two steps. First, by irradiation at 254 nm, anthracene dimers were de-crosslinked to liquefy the material around the scratches. Then by irradiation with 366 nm light, the crosslinks were restored again and the scratches were disappeared.

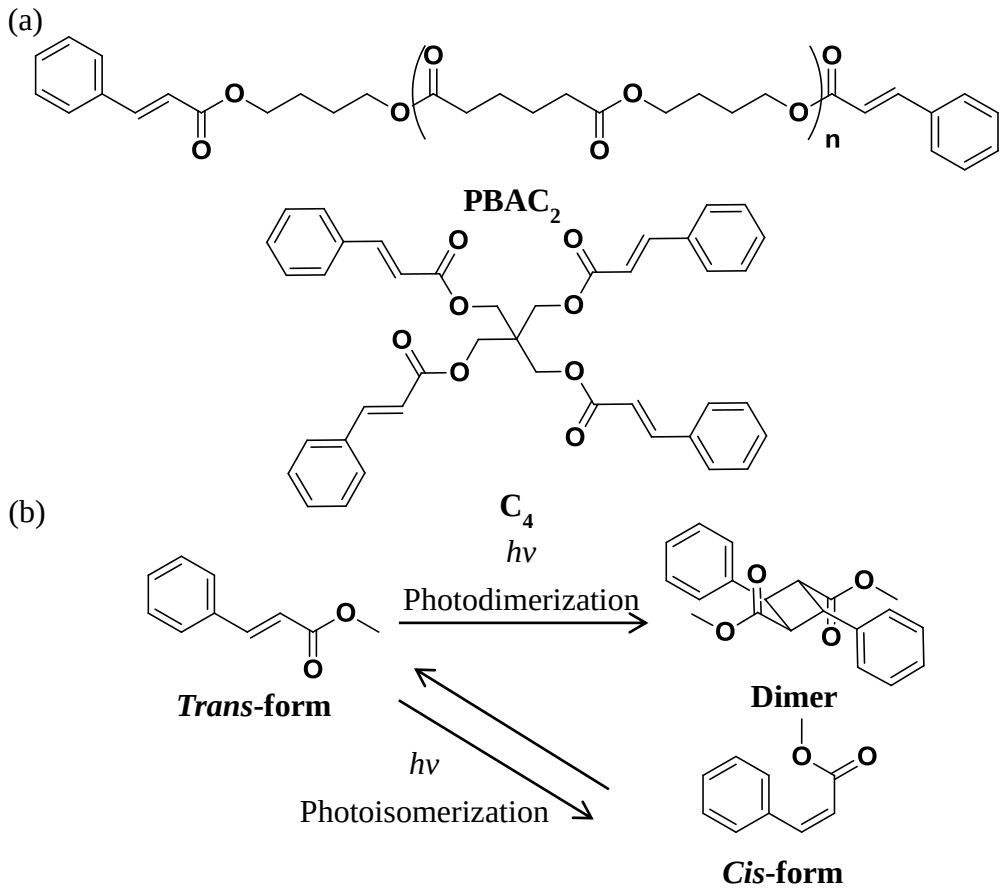

Figure 2-2 Molecular structures of $PBAC_2$ and C_4 (a) and photo reactions of cinnamate (b).

In this chater, the author synthesized a photoinduced mendable network polymer from a cinnamoyl-telechelic poly(butylene adipate), $PBAC_2$ and a tetra-cinnamoyl linker, C_4 connected via photodimerization of cinnamoyl groups (Figure 2-2). The main chain of the telechelics determines the basic performance of the polymers while the functionalities of them are regulated by the reversible groups. So, the functionalities and the basic performance can be designed independently in these network polymers. Photo-polymerization and photo-mending behavior are analyzed by UV/Vis and ATR-IR spectroscopies.

Experimental section

Materials. Poly(butylene adipate) diol (PBAdiol, M_n^{NMR} = 1000. GPC: M_n^{GPC} = 1010; M_w/M_n = 3.28) was obtained from Aldrich. Pentaerythritol and cinnamoyl chloride were purchased from Tokyo Chemical Industry CO. Ltd. Chloroform and methanol were purchased from Wako Pure Chemical Industries, Ltd. Ethanol were purchased from Nacalai Tesque, Inc. Anhydrous tetrahydrofuran was purchased from Kanto Chemical Co. All reagents and solvents were used as received.

Synthesis of cinnamoyl-telechelic poly(butylene adipate), [PBAC$_2$]. PBAdiol (2.81 g) and cinnamoyl chloride (7.07 g, 15 e.q.) were dissolved in dehydrated THF (40 mL) with N_2 purging and stirred under reflux for three days. After cooling to room temperature, the product was precipitated with excess ethanol at 0 ^oC and dried under vacuum. Cinnamoyl-terminated PBA was obtained after dissolution in $CHCl_3$, followed by precipitation with methanol at 0 ^oC and dried under vacuum. The yield was 1.074 g. ^{1}H-NMR [$CDCl_3$], δ/ppm 1.64-1.79 (m, CH_2, overlapped with H_2O peak), 2.33 (m, CH_2), 4.09-4.24 (m, CH_2), 6.46 (d, CH), 7.55-7.38 (m, aromatic), 7.71 (d, CH), M_n^{NMR} = 2900, from the relative areas of the cinnamate peak at 6.46 ppm and the PBA peak at 2.33 ppm. GPC: M_n^{GPC} = 4500; M_w/M_n = 1.27.

Synthesis of pentaerythritol tetracinnamate, [C$_4$]. Mixture of pentaerythritol (0.163 g, 1.2 mmol) and cinnamoyl chloride (1.00 g, 6.0 mmol) was kept at 120 ^oC for 3 hours. After cooling, the crude product was solved in hot ethanol and recrystallized from it. After filtration, product was obtained (1.92 g, 49% yield). ^{1}H-NMR [$CDCl_3$], δ/ppm δ4.47 (s, 2H)), 6.46 (d, 1H), 7.35 (m, 3H), 7.49 (m, 2H), 7.71 (d, 1H); FAB-MS:

657.4 (MH), $C_{41}H_{36}O_8$, calcd 656.24. DSC: T_m=126 ^oC.

Photopolymerization of $PBAC_2$ and C_4. Thin films of $PBAC_2$, C_4 and 1/1 (mol/mol) mixture of them were prepared on quartz plates by spin-coating from dilute chloroform solution at spinning rate of 2000 rpm. The films were photo-irradiated at a wavelength band of 300-400 nm by using a 100 w xenon lamp (LAX-Cute, Asahi spectra Co. Ltd.) with a UVA mirror module.

Mendability test. Spin-coated film (thickness ≈ 0.01 mm) of 1/1 $PBAC_2/C_4$ on quartz was polymerized by photoirradiation at 300-400 nm for 10 minutes at 60 ^oC. The film was then covered with a thin glass plate (Matsunami Glass Ind.,Ltd, micro cover glass No. 1) and tapped with fingers gently to avoid breaking the glass for many times. To the tapped film, light of 300-400 nm was applied again for 10 minutes at 60 ^oC. On each step, UV/Vis absorption spectrum was collected.

Analytical Procedures. UV/Vis absorption spectra were collected on a U-3010 Hitachi spectrophotometer. GPC measurements were performed on a Tosoh HLC 8220 GPC system equipped with two TSK-Gel GMH_{HR}-N columns ($CHCl_3$, 40 °C, 1 $mg \cdot mL^{-1}$). Polystyrene standards with low polydispersity were used to construct a calibration curve. ^1H NMR spectra of chloroform-*d* solutions were measured by using JEOL JNM-ECS400 NMR SYSTEM at room temperature. FAB-MS measurements were performed on a JEOL JMS-600H. Attenuated total reflection (ATR) IR spectroscopy was measured with Thermo Scientific Nicolet iS10 equipped with Smart iTR accessory with ZnSe crystal. Differential scanning calorimetry (DSC) was carried out on a Perkin

Elmer Pyris 1 under a N_2 atmosphere. Samples in aluminum pans were measured. Melting point (T_m) and heat of fusion (ΔH_f) were taken as the peak top and area of melting endotherm during heating at a rate of 10 °C min^{-1} after crystallization at 20 ^oC for 4 min. Heat flow during isothermal crystallization was also observed at 28 °C. All samples were first thermally treated at 60 °C and quenched to the crystallization temperature.

Results and Discussion

Photoreaction of $PBAC_2$, C_4 and their 1/1 mixture(UV/Vis)

Photoreactivity of the cinnamoyl groups of 1/1 $PBAC_2$ / C_4 mixture in the bulk state was monitored by UV/Vis absorption spectroscopy.

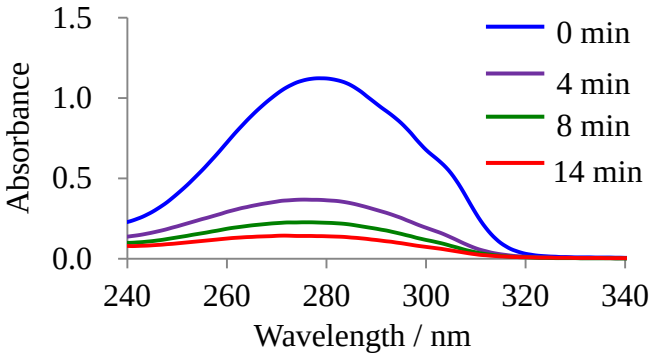

Figure2-3 UV-Vis spectra of 1/1 (mol/mol) $PBAC_2/C_4$ film on quartz during photoirradiation (λ=300~400 nm) at 60 ^oC for 0, 4, 8 and 14 min.

Figure2-3 shows the time course of the UV/Vis absorption spectra for the 1/1 (mol/mol) mixture of $PBAC_2$ and C_4 during photoirradiation (λ =300-400 nm) at 60 ^oC. The absorption at 280 nm, coming from the cinnamoyl group, reduced with irradiation time, indicating that the dimerization of the cinnamoyl groups was promoted by photoirradiation.

Photoreaction of $PBAC_2$, C_4 and their 1/1 mixture(ATR-IR)

ATR-IR spectroscopy also shows the formation of the cinnamoyl dimers (Figure 2-4). In the spectra of the 1/1 mixture of $PBAC_2$ and C_4 before photoirradiation, the C=C and C=O stretching bands of the cinnamoyl group appear at 1636 cm^{-1} and 1716 cm^{-1} (as a shoulder), respectively[17]. After irradiation at 300-400 nm light for 10 minutes, these

characteristic peaks were disappeared, indicating the comsumption of the cinnamoyl groups to form dimers.

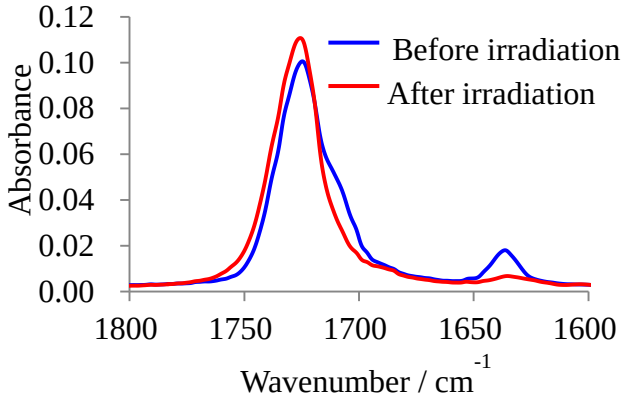

Figure 2-4 Changes of ATR-IR spectra of 1/1 $PBAC_2/C_4$ by photoirradiation at 60 ^oC; before irradiation (blue line), after irradiation for 10 min (red line).

Fractional populations of *trans-cis* isomers and dimer of cinnamoly groups

It is well known that cinnamate is in *trans*-form under ambient conditions. By irradiation with UV light, both the dimerization via [2+2] cycloaddition and the isomerization to *cis*-form occur (see Figure 2-2). While the dimer has no absorption peaks between 250-350 nm, both the *trans*- and *cis*-monomers have absorption peaks at around 280 nm. If the *trans-cis* isomerization solely proceeds, an isosbestic point appears at 250 nm[18]. Disappearance of the isosbestic point in the spectra clearly shows that the dimerization competed with the isomerization in the sample during the photoirradiation (Figure 2-3).

The UV/Vis absorption spectra can be analyzed quantitatively based on the following equations[19];

$$f_{\mathrm{T}} = \frac{\varepsilon_{\mathrm{T}}}{\varepsilon_{\mathrm{T}}-\varepsilon_{\mathrm{C}}}\left(\frac{{D_{max}}^{t}}{{D_{\mathrm{max}}}^{0}} - \frac{\varepsilon_{\mathrm{C}}{D_{\mathrm{iso}}}^{t}}{\varepsilon_{\mathrm{T}}{D_{\mathrm{iso}}}^{0}}\right) \quad (1)$$

$$f_{\mathrm{C}} = \frac{\varepsilon_{\mathrm{T}}}{\varepsilon_{\mathrm{T}}-\varepsilon_{\mathrm{C}}}\left(\frac{{D_{\mathrm{iso}}}^{t}}{{D_{\mathrm{iso}}}^{0}} - \frac{{D_{\mathrm{max}}}^{t}}{{D_{\mathrm{max}}}^{0}}\right) \quad (2)$$

$$f_{\mathrm{D}} = \left(1 - \frac{{D_{\mathrm{iso}}}^{t}}{{D_{\mathrm{iso}}}^{0}}\right) \quad (3)$$

where subscripts T, C, and D denote the *trans*-cinnamate, *cis*-cinnamate, and dimer, respectively; *f* is the mole fraction; ε is the molar extinction coefficients at 271 nm. ${D_{\mathrm{iso}}}^{t}$ and ${D_{\mathrm{max}}}^{t}$ are, respectively, the optical densities at 250 nm (isobestic point of isomerization) and 271 nm at time *t*. Using these equations and the extinction coefficients data from Rennert *et al.*[20], the progress of the dimerization and isomerization in 1/1 $PBAC_2/C_4$ at 60 °C was estimated as shown in Figure 2-5. Initially the isomerization to *cis*-form proceeded quickly, followed by the gradual progress of dimerization. The photoreaction reached stationary state in 14 min, where the dimer becomes the major product.

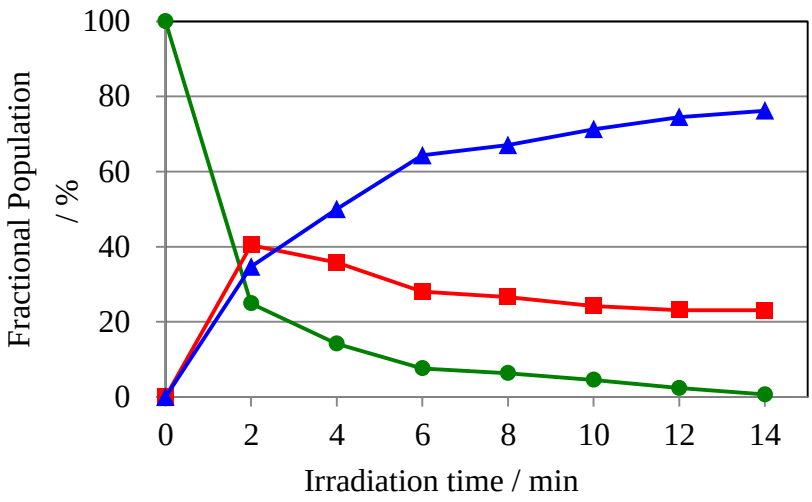

Figure2-5 Simultaneous progress of cycloaddition and *trans-cis* isomerization in 1/1 $PBAC_2/C_4$ during photoirradiation; fractional populations of *trans*-cinnamate (circle), *cis*-cinnamate (square), and dimer (triangle) are plotted as a afunction of irradiation time.

The photopolymerizations in pure $PBAC_2$ and that at room temperature was also analyzed. The irradiation time required to reach photostationary state and the fractional populations of the dimer and two isomeric monomers in that state are summarized in Table 2-1.

Table 2-1. Fractional populations of *trans* and *cis*-isomers and dimer of cinnamoly groups in the photostationary state

Entry	Sample	Photoreaction Temp.	Time to reach stationary state / s	*Trans* / %	*Cis* / %	Dimer / %
1	$PBAC_2$	r.t.	540	13	55	32
2	$PBAC_2$	60 ^oC	2100	1	31	68
3	1/1 $PBAC_2/C_4$[(a)]	r.t.	420	41	16	43
4	1/1 $PBAC_2/C_4$[(a)]	60 ^oC	840	1	23	76

(a): Mixture of $PBAC_2$ and C_4 in 1:1 molar ratio

The cinnamate dimer was the main component of the photoreactions at 60 ^oC (Entry 2, 4), while more *trans*- and *cis*-monomers remained in the stationary state at room temperature (Entry 1, 3). This temperature dependence can be explained by the difference in the molecular mobility. The melting point of $PBAC_2$ is 44 °C. At a temperature below this melting point, encounter of cinnamoyl groups is restricted, which promotes the progress of isomerization. More *trans*-monomers existed in 1/1 $PBAC_2/C_4$ (Entry 3) than in $PBAC_2$ (Entry 1). Since four cinnamoyl groups are crowded in C_4, *cis*-isomers might be less preferable sterically at room temperature. On

the other hand, higher molecular mobility in the melt $PBAC_2$ assists the dimerization. At each temperature, 1/1 $PBAC_2/C_4$ reached the stationary state faster than pure $PBAC_2$. The stationary state of 1/1 $PBAC_2/C_4$ contained more dimer than that of $PBAC_2$. These resutls can be explained by the difference in the concentration of cinnamoyl groups, which is calculated from the molecular weight of $PBAC_2$ (M_n^{NMR} = 2900) and C_4 (M.W. = 656). Only one mole of cinnamoyl groups are contained in 1500 g of pure $PBAC_2$ while 600 g of 1/1 $PBAC_2/C_4$ contains one mole of cinnamoyl groups. The higher concentration allowed more encounters between two monomers, which promots the dimerization.

Network polymer formation from $PBAC_2/C_4$ mixture

The formation of network structure in the photopolymerized samples was examined by solubility test(Figure 2-5).

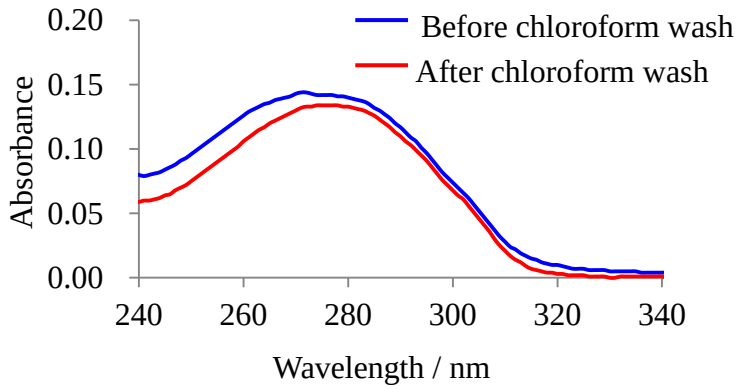

Figure2-6 UV-Vis spectra of photodimerized 1/1 $PBAC_2/C_4$ film before and after chloroform wash.

When the photoreacted film of pure $PBAC_2$ was immersed in chloroform, the sample

was completely washed away. Only the linear polymer of PBA is synthesized by this photopolymerization. On the other hand, the photoreacted film of 1/1 $PBAC_2/C_4$ were hardly dissolved in chloroform. After the immersion of this film to chloroform, the intensity of the UV/Vis absorption did not change compared with the absorption before immersion (Figure 2-6). An insoluble network structure was formed by dimerization of the cinnamoyl groups in this mixture. The photodimerization in 1/1 $PBAC_2/C_4$ surely links $PBAC_2$ and C_4 to form the network structure though cinnamoyl dimers must be also formed between two C_4 linkers and between two $PBAC_2$ prepolymers.

Thermal properties of 1/1 $PBAC_2/C_4$.

Isothermal crystallization of $PBAC_2$ before and after photoirradiation and 1/1 $PBAC_2/C_4$ after photoirradiation was observed at 28 ^oC after quenching from the molten state (Figure 2-7(a)). The crystallization of $PBAC_2$ both before and after photoirradiation completed within 0.5 min while that of 1/1 $PBAC_2/C_4$ after photoirradiation takes 3 min. This slow crystallization indicates that photodimerization surely occured between cinnamoyl groups of $PBAC_2$ and C_4 to form network structures. These crosslinks make crystallization of PBA slower.

Figure 2-7(b) shows DSC heating curves of photopolymerized 1/1 $PBAC_2/C_4$ crystallized from melt at 20 ^oC for 4 min. The curve had three endothermaic peaks. The heating scans with various heating rates showed that the highest temperature peak is ascribable to the melt–recrystallization during the heating scan. The middle temperature peak at 43 ^oC corresponds to the melting point of PBA ($T_m \approx 48\ ^oC$). Photodimerization between $PBAC_2$ gives long linear chain, which forms crystals similar to pure PBA. The lowest temperature peak at 36 ^oC can be ascribed to the melting of PBA near the

crosslinks made by photoreaction of $PBAC_2$ and C_4.

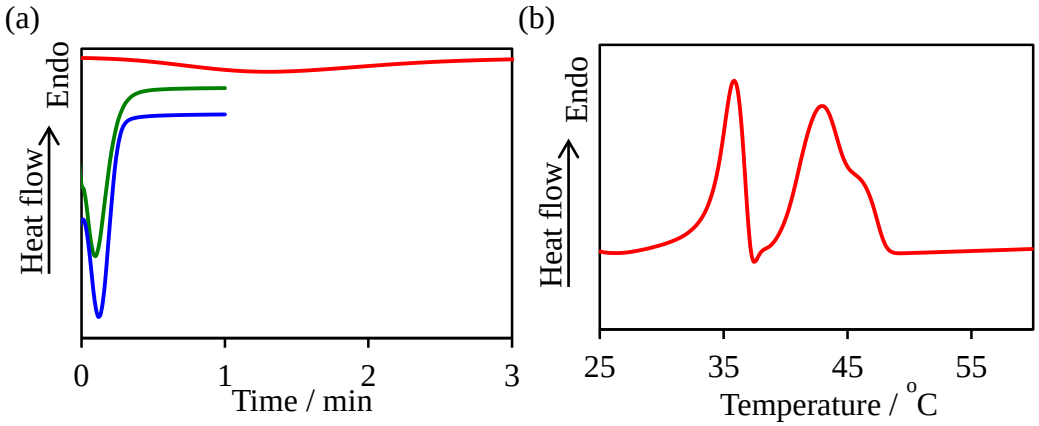

Figure2-7 (a) DSC curves during isothermal crystallization at 28 ^{o}C of $PBAC_2$ before(blue line) and after(green line) photopolymerization and 1/1 $PBAC_2/C_4$ after photopolymerization(red line). (b) DSC curves of photopolymerized 1/1 $PBAC_2/C_4$ during heating at a rate of 10 ^{o}C min^{-1}.

Mendability of photopolymerized 1/1 $PBAC_2/C_4$.

Mending ability of 1/1 $PBAC_2/C_4$ was analyzed through the comparison of UV/Vis spectra of the samples *as-cast*, *as-polymerized*, *as-damaged*, and *as-mended* by photoirradiation.

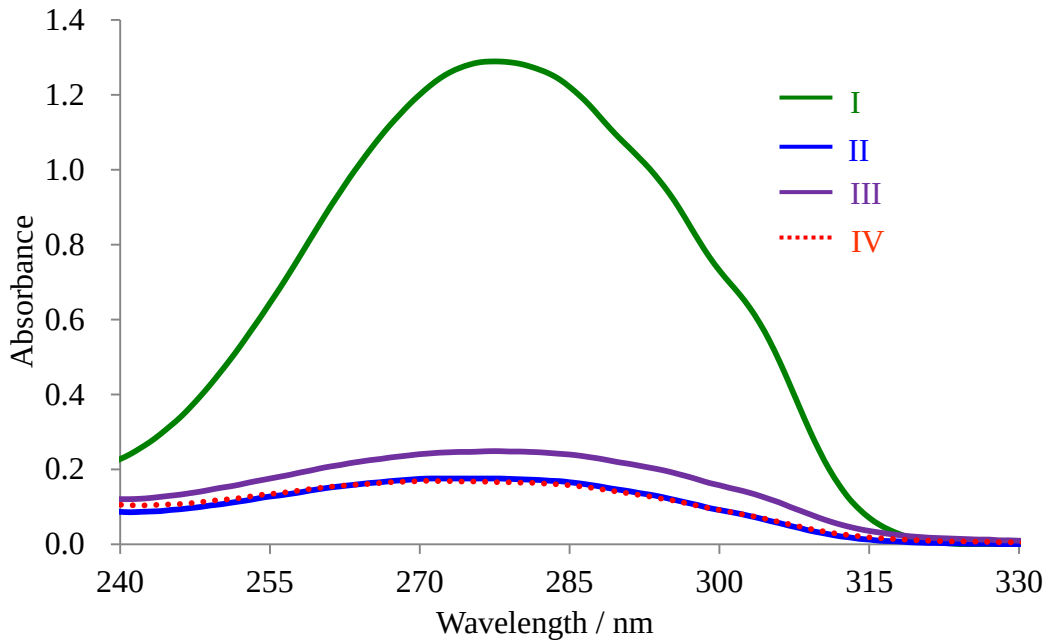

Figure2-8 UV/Vis spectra of 1/1 $PBAC_2/C_4$ of *as-cast* (I), *as-polymerized* (II), *as-damaged* (III), and *as-mended* (IV).

The spectra is shown in Figure 2-8. Figure 2-9 shows schematic representation of mending mechanism in $PBAC_2/C_4$. First, spin-coated film (thickness ≈ 0.01 mm) of 1/1 $PBAC_2/C_4$ was prepared. In the UV/Vis absorption spectrum of this film (I),

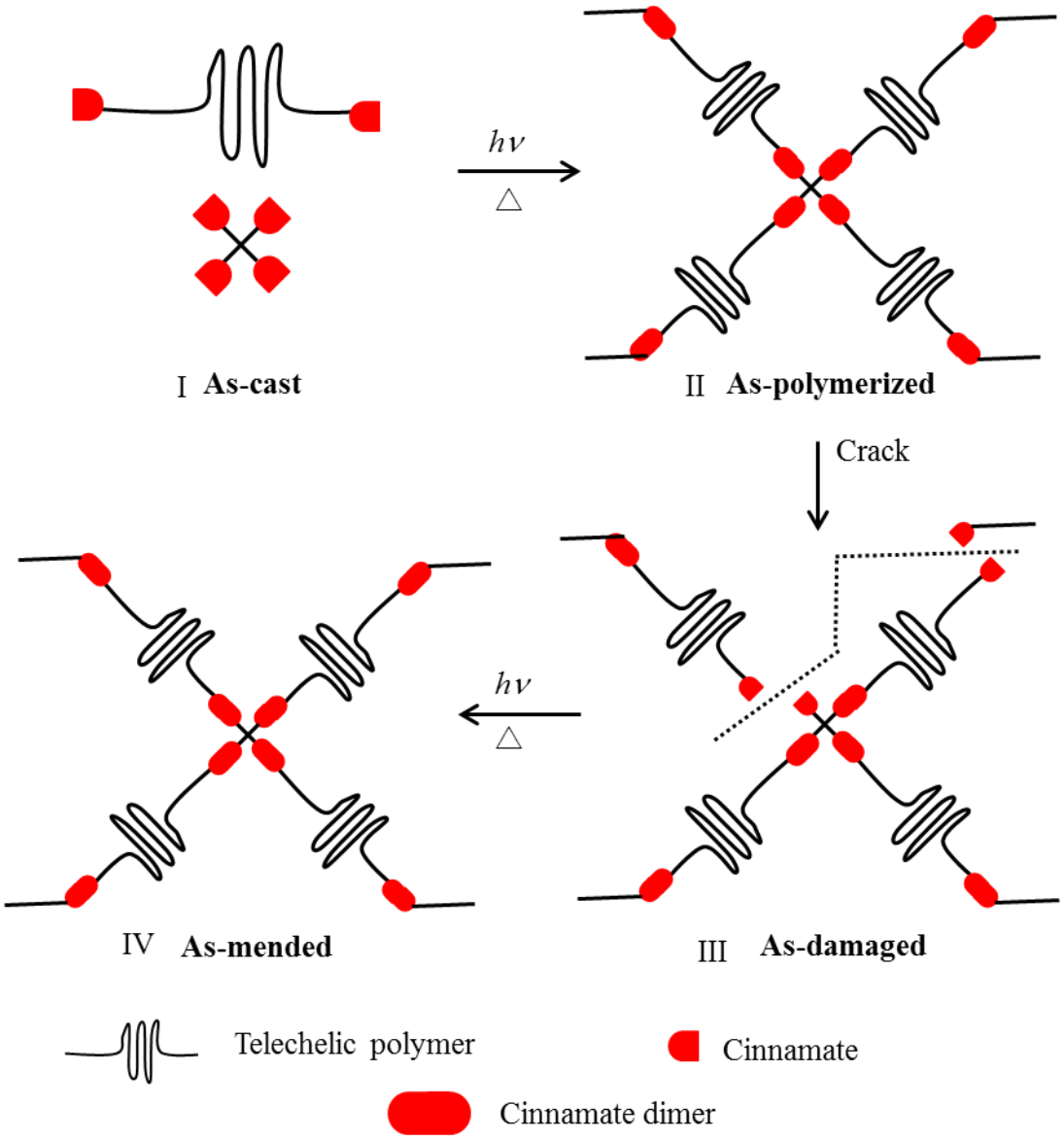

Figure 2-9 Schematic representation of mending mechanism in $PBAC_2/C_4$.

the characteristic peak of cinnamate was observed at 280 nm. When the film was photoirradiated with light of 300-400 nm for 10 minutes at 60 ^{o}C, the cinnamate absorbance was significantly decreased (II), indicating the progress of photodimerization reaction. This photodimerized polymer film was then covered with a glass plate and damaged by tapping with fingers for many times. The cinnamate absorbance at 280 nm slightly increased again (III), indicating the partial cleavage of cyclobutane structure in the dimer to the original cinnamate structure. Because of the large ring strain, the cyclobutane structure is so fragile to be broken by mechanical stress. To the damaged film, light of 300-400 nm was applied again for 10 minutes at 60 ^{o}C. The absorbance at 280 nm reverted back to the intensity before tapping (IV), indicating that cinnamate groups in the damaged film were dimerized to form cyclobutane rings again. These results demonstrate the photoreversible mending property of the PBAC_2/C_4 system.

Table 2-2 Change in the fractional populations of isomers and dimer of cinnamoly groups during mending experiment

Step	*Trans* (%)	*cis* (%)	dimer (%)
I	100	0	0
II	3	20	77
III	3	30	67
IV	0	26	74

The progress of dimerization during this mending process was calculated based on Eqs. 1-3. The fractional poputlations of the dimer and two isomeric monomers at each stage are summarized in Table 2-2. By the first photoirradiation, the amount of the *trans*-monomer reduced to 3 % and those of the dimer and the *cis*-monomer grew to 77 % and 20 %, respectively (II). Damaging the sample resulted in the cleavage of the cyclobutane rings to generate *cis*-cinnamate (III). Ten percent of the dimer was monomerized to the *cis*-forms. By the re-irradiation, the dimerization proceeded again (IV). The amount of the dimer recovers to 74 %. Therefore, the cyclobutane rings broken by the mechanical stress can be repaired by photoirradiation in the $PBAC_2/C_4$ system. Recovery of the broken covalent bonds by photoirradiation can repress the macro crack formation. Additionally, during this damaging and mending process, the dimers located elsewhere than the damaged part remains intact. Monomerization of the dimers is not required for the progress of the mending process. This robust structure allows for the maintenance of the sample shape.

Conclusion

A telechelic prepolymer having cinnamate end groups, $PBAC_2$, and pentaerythritol tetracinnamate, C_4, were synthesized and crosslinked by photodimerization of the cinnamoyl groups to obtain a network polymer, $PBAC_2/C_4$. Progress of the crosslinking reaction was analyzed by UV/Vis and IR spectroscopy. Though *trans-cis* isomerization of the cinnamoyl group competes with dimerization, more dimerization proceeds at a temperature higher than the melting point of $PBAC_2$. The mending behavior of the network polymer was also analyzed by UV/Vis spectroscopy. When the crosslinked $PBAC_2/C_4$ is damaged, the cinnamate dimers at the crack surfaces are dissociated to generate cinnamate monomers. Photoirradiation of the damaged sample lead the re-dimerization of cinnamate monomers at the crack surfaces to mend the network polymer. This mending process allows to recover the chemical structure of the polymer completely. Tough the prepolymer used in this study was telechelics of PBA, various photomendable polymers can be obtained by simply replacing the main chain of the telechelics.

Reference

[1]a) D. Y. Wu, S. Meure and D. Solomon, *Prog. Polym. Sci.*, **2008**, *33***,** 479; b) E. B. Murphy and F. Wudl, *Prog. Polym. Sci.*, **2010**, *35*, 223.

[2]a) S. R. White, N. R. Sottos, P. H. Geubelle, J. S. Moore, M. R. Kessler, S. R. Sriram, E. N. Brown and S. Viswanathan, *Nature*, **2001**, *409*, 794, b) B. J. Blaiszik, M. M. Caruso, D. A. McIlroy, J. S. Moore, S. R. White and N. R. Sottos, *Polymer*, **2009**, *50*, 990, c) M. W. Keller, S. R. White and N. R. Sottos, *Adv. Func. Mater***.**, **2007**, *17*, 2399.

[3]a) X. X. Chen, M. A. Dam, K. Ono, A. Mal, H. B. Shen, S. R. Nutt, K. Sheran and F. Wudl, *Science*, **2002**, *295*, 1698, b) E. B. Murphy, E. Bolanos, C. Schaffner-Hamann, F. Wudl, S. R. Nutt and M. L. Auad, *Macromolecules*, **2008**, *41*, 5203.

[4]C. M. Chung, Y. S. Roh, S. Y. Cho and J. G. Kim, *Chem. Mater***.**, **2004**, *16*, 3982.

[5]G. Deng, C. Tang, F. Li, H. Jiang and Y. Chen, *Macromolecules*, **2010**, *43*, 1191.

[6]P. Cordier, F. Tournilhac, C. Soulie-Ziakovic and L. Leibler, *Nature*, **2008**, *451*, 977.

[7]Q.Wang, J. L. Mynar, M. Yoshida, E. Lee, M. Lee, K. Okuro, K. Kinbara, and T. Aida, *Nature*, **2010**, *463*, 339.

[8] S. Burattini, H. M. Colquhoun, J. D. Fox, D. Friedmann, B. W. Greenland, P. J. F.

Harris, W. Hayes, M. E. Mackay and S. J. Rowan, *Chem. Commun.*, **2009**, 6717.

[9] B. Ghosh and M. W. Urban, *Science*, **2009**, *323*, 1458.

[10]. D. H. Suh., Y. Hayashi., K. Ichimura, *Macromol Chem Phys* **1998**, *199*, 363.

[11]. (a) M. Obi, S. Morino, K. Ichimura, *Macromol. Rapid Commun.* **1998**, *19*, 643. (b) P. O. Jackson, M. O'Neil, *Chem. Mate.* **2001**, *13*: 694.

[12]. T. Li, J. Chen, M. Mitsuishi and T. Miyashita, *J. Mater. Chem.*, **2003,** 3565.

[13]. (a) H. Kihara and N. Tamaoki, *Liquid Crystals.* **2007**, *34*. 1337. (b) S. Furumi and K. Ichimura, *J. Phys. Chem. B*, **2007,** *111*, 1277.

[14].N. Kawatsuki, K. Goto, T. Kawakami, and T. Yamamoto, *Macromolecules* **2002,** *35*, 706.

[15].C. M. Chung, Y. S. Roh, S. Y. Cho, J. G. Kim, *Chem. Mater.* **2004**, *16*, 3982.

[16]. P. Froimowicz, H. Frey, K. Landfester, *Macromol. Rapid Commun*. **2011**, 32, 468.

[17]. A. H. Ali, K. S. V. Srinivasan, *Polymer Int.* **1997**, *43*, 310.

[18]. Y. Nakayama, T. Matsuda, *J. Polym Sci.: Part A: Polym. Chem.*, **2005**, 43, 3324.

[19]. L. Egerton, E. Pitts, A. Reiser, *Macromolecules* **1981**, *14*, 95.

[20]. J. Rennert, S. Soloway, I. Waltcher, B. Leong, *J. Am. Chem. Soc.* **1972**, *94*, 7242.

Chapter 3.

Crystalline polymers with mending ability at room temperature

3-1 General introduction of Chapter3

Described in Chapter2, polymers having capability to repair these cracks during their duration of service are recently attracted much attention, because mending properties are valuable to extend the working life and to enhance the safety performance of polymer materials.[1]

For mendable polymer constructed by dynamic bonds[2,3], molecular mobility is critical for the mending processes because repairing occurs by the reformation of dynamic bonds between crack surfaces. Actually, in previous papers, mending ability at room temperature was realized in gels or soft elastic polymers with good molecular mobility.[3] Mending in more rigid polymers is achieved by applying some external stimuli to promote the cleavage of the dynamic bonds[2,4] and/or the melting of the polymer crystals[5], like Chapter2. It is difficult to obtain crystalline polymers with mending ability at room temperature.

In this chapter, the author introduces a new approach to prepare crystalline polymers with mending ability at room temperature, or mendable polymers which keep the bulk crystallinity phase throughout the mending process. This approach relies on the control of crystallization. When a crystalline polymer is mechanically broken, the degree of crystallinity at the crack surface is more or less decreased by frictional heat, which results in the higher molecular mobility near the crack location. Though the degree of crystallinity at the crack surface is recovered with time by recrystallization, mending mechanism may proceed in the undercooled state if the crystallization is sufficiently slow.

3-2 Construction of crystalline polymers with mending ability at room temperature

Introduction

Supramolecular interaction based on ureidopyrimidinone [UPy] units was employed in some mending polymers.[6] Because of its quadruple hydrogen-bonding nature, the UPy units at the chain ends contribute to the formation of supramolecular polymer with high degrees of polymerization. Poly(ethylene adipate) [PEA] is a semicrystalline polyester with melting point at 45 °C. The author has chosen UPy and PEA as the dynamic bond and the polymer matrix of the mendable crystalline polymer. The author attempted to slow down the crystallization of this polymer by inserting a bulky tolylene unit between UPy and PEA. Actually, as described latter, this polymer is a slow crystallizing polymer with a repeatable mending ability at room temperature.

Experimental section

Materials.

2-Amino-4-hydroxy-6-methylpyrimidine, hexamethylene Diisocyanate, and dibutyltin dilaurate were purchased from Tokyo Chemical Industry CO. Ltd. Tolylene 2,4-diisocyanate terminated Poly(ethylene adipate) were purchased from Aldrich. Adipic acid and ethylene glycol were purchased from Nacalai tesque, Inc. Chloroform and methanol were purchased from Wako Pure Chemical Industries, Ltd. Anhydrous solvents of chloroform was purchased from Kanto Chemical Co. All reagents and solvents were used as received.

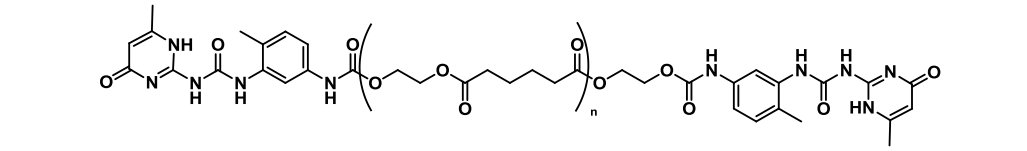

PEA-toly-UPy

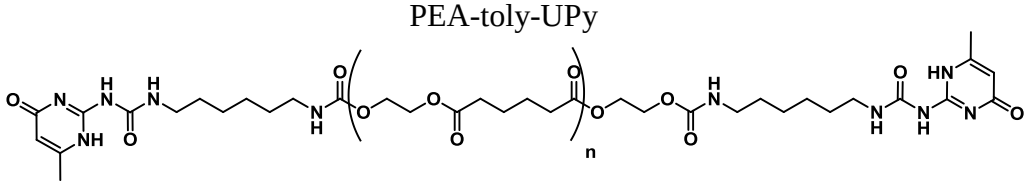

PEA-hexy-UPy

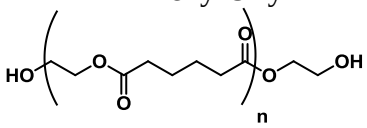

PEA-diol

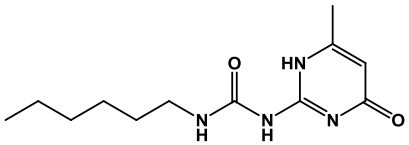

Hexy-UPy

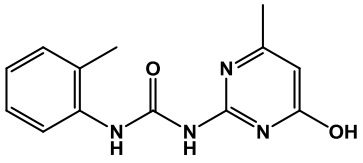

o-toly-UPy

Figure 3-2-1 Chemical structures of telechelic polymers, inhibitor of supramolecular interaction and a model molecule

Synthesis of UPy-tolylene-telechelic poly(ethylene adipate) [PEA-toly-UPy].

Under N_2 atmosphere, tolylene-2,4-diisocyanate-terminated poly(ethylene adipate) (6.182 g) and 2-amino-4-hydroxy-6-methylpyrimidine (1.720 g/excess) was dissolved in 60 ml of dehydrated chloroform. The reaction mixture was stirred for 22 h under reflux and then cooled down to room temperature. 30 ml of *N*,*N*-dimethylformamide was added to the mixture and then chloroform was removed from the mixture by evaporation. The product was obtained by filtration and precipitation with excess water at room temperature and dried under vacuum at 80 °C. The yield was 5.830 g. ATR-IR (cm^{-1}): 3339, 2955, 1731, 1620, 1600, 1445, 1384, 1279, 1137, 823-2H NMR: [$CDCl_3$], δ/ppm 1.67 (br, CH_2), 2.22 (s, CH_3), 2.28 (s, CH_3), 2.36 (br, CH_2), 4.27-4.33 (m, CH_2), 5.83 (s, CH), 6.71 (br, NH), 7.13–8.00 (m, aromatic, overlapping $CHCl_3$ peaks), 11.79 (br, CH), 12.36 (br, NH), 12.99 (br, NH). ^{13}C NMR: δ/ppm 17.16, 18.94, 23.91, 33.43, 62.41, 62.70, 106.90, 117.01, 126.45, 131.06, 135.09, 136.47, 148.68, 151.85, 153.09, 154.58, 172.86, 173.01. M_n^{NMR} = 5900. The terminal modification rate of PEA in PEA-toly-UPy is 74% and the remaining 26 % are primary amine terminals generated by the hydrolysis of isocyanate group. PEA-toly-UPy with M_n^{NMR} = 5700 and terminal modification rate of 82% was used for viscometric measurements and tensile tests, and another(M_n^{NMR} = 3300, terminal modification rate of 84%) for mending experiments of recovery rates.

Synthesis of poly(ethylene adipate) diol [PEA-diol].

PEA-diol was synthesized by a two-step polycondensation reaction as follows. A mixture of adipic acid and ethylene glycol with the molar ratio of adipic acid / ethylene glycol = 1/1.1 was melted and stirred at 170 °C for 2 h with exclusion of water. The

reaction mixture was stirred at 170 °C under a reduced pressure (<2 mmHg) for 4 h. After cooling to room temperature, the product was dissolved in chloroform, precipitated with methanol at 0 ^{o}C and dried under vacuum. M_n^{GPC} = 2000, M_w/M_n = 2.3-2H NMR: [$CDCl_3$], δ/ppm 1.67 (br, CH_2),2.37 (br, CH_2), 3.83 (t, CH_2), 4.22 (t, CH_2), 4.27 (br, CH_2), M_n^{NMR} = 4500.

Synthesis of UPy-hexyl-telechelic poly(ethylene adipate) [PEA-hexy-UPy]

UPy-Hex-PEA was obtained by a modification of end groups of PEA-diol by a procedure similar to the one described in a previous paper[6(b)]. M_n^{NMR} = 5100. The terminal modification rate of PEA in PEA-hexy-UPy was 94% and 6 % of hydroxyl terminals remain.

Synthesis of *N*-Hexyl-*N*-(1,4-dihydro-4-oxo-6-methyl-2-pyrimidinyl)-urea [Hexy-UPy]

Hexy-UPy was synthesized as previously reported as an inhibitor of the supramolecular chain extension of PEA-UPys(PEA-hexy-Upy and PEA-toly-Upy).[7]

Synthesis of *N*-[(m-tolylamino)carbonyl]-6-methylisocytosine, [o-toly-UPy]

Under N_2 atmosphere, m-tolyl isocyanate (1.185 g, 8.91 mmol) and 2-amino-4-hydroxy-6-methylpyrimidine (1.025 g, 8.20 mmol) was dissolved in 20 ml of dehydrated N,N-dimethylformamide. The reaction mixture was stirred for 1 day at 80 ^{o}C and then cooled down to room temperature. Precipitate was filtered and washed by N,N-dimethylformamide and following waster. Precipitate was dried in vacuum at 80 ^{o}C and white solid (1.588 g) was obtained. (400 MHz, $CDCl_3$-*d*) 3-2 (s, CH_3), 2.2 (s, CH_3),

5.8 (s, CH) , 7.1-7.23 (m, overlapped with $CHCl_3$ peak), 11.8(br, CH), 12.5(br, NH), δ13-2(br, NH) From ^{1}H-NMR spectrum, this compound was not pure and purity was 80 %. FAB-MS: 259.2 (MH), $C_{13}H_{14}N_4O_2$, calcd258.11

Analytical Procedures.

^{1}H NMR spectroscopy was performed using JEOL JNM-ECS400 NMR SYSTEM. The number average molecular weight of PEA-toly-UPy was estimated by comparing the peak areas of CH_2 of PEA(4.27-4.33 ppm) and CH_3 of the tolylene unit(2.28 ppm). The terminal modification rate of PEA-toly-UPy was estimated by comparing the CH_3 peak areas of the tolylene (2.18 ppm) and UPy units(2.23 ppm), measured in DMSO-*d6*.
The number average molecular weight of PEA-diol was estimated by comparing the peak areas of PEA(4.28 ppm) and the hedroxy methyl end groups(CH_2) at 3.83 ppm.
The number average molecular weight of PEA-hexy-UPy was estimated by comparing the peak areas of PEA(4.26 ppm) and UPy unit(5.83 ppm). The terminal modification rate of PEA-hexy-UPy was caluculated by comparing the peak areas of the hedroxy methyl end groups(CH_2) of PEA(3.83 ppm) and UPy unit(5.83 ppm).
Gel permeation chromatography (GPC) was carried out using Tosoh HLC 8220 GPC system equipped with TSK-Gel GMH_{HR}-N columns ($CHCl_3$, 40 ^{o}C, 1 mg mL^{-1}). Polystyrene standards with low polydispersity were used to construct a calibration curve.
Differential scanning calorimetry (DSC) was carried out with Perkin-Elmer Pyris 1 at a heating rate of 10 ^{o}C/min under a N_2 atmosphere. Melting temperature, T_m, and heat of fusion, ΔH_f, was taken as the peak top and the area of the melting endotherm,

respectively. The crystallinity of PEA-UPys was calculated by dividing ΔH_f of the sample with theoretial ΔH_f value of PEA-diol with 100% crystallinity.

Mechanical properties of film samples were evaluated using a tensile testing machine, SHIMAZU EZ test, at a cross-head speed of 10 mm min^{-1} at room temperature. The dumbbell specimens of samples (with the center section 1.4 mm wide, 7.0 mm long and 0.3-0.5 mm thick) were used. Values of Young modulus, stress at yield, and elongation at break were averaged over the data of at least three specimens. Recovery rates were calculated from tensile tests at a cross-head speed of 50 mm min^{-1} at room temperature. The rectangle specimens of samples (with the center section 5 – 5.5 mm wide, 7.0 mm long and 1.65 - 1.81 mm thick) were used.

Attenuated total reflection infrared (ATR-IR) spectroscopy was measured with Thermo Scientific Nicolet iS10 equipped with Smart iTR accessory with ZnSe crystal. The IR spectra were recorded over a spectral range from 650 to 4000 cm^{-1} with a resolution of 4 cm^{-1}.

Rheology measurements were carried out with a TA Instrument $AR2000_{ex}$ at a frequency of 1 Hz and a heating rate of 5 ^oC min^{-1}. PEA-toly-UPy films of 10 mm×10 mm×0.36 mm were measured.

Viscosity measurement was carried out using A&D company SV-1A. A solution containing 1.2 g of PEA-toly-UPy in 30 ml of $CHCl_3$ were measured at 28.0 °C. A solution containing 1.2 g of PEA-toly-UPy and 86.5 mg of Hexy-UPy (molar ratio of UPy in PEA-toly-UPy to UPy in Hexy-UPy = 1:1) was measured at 26.5 °C. The results were averaged over the data of at least three samples. Sollution densities were measured by A&D company GX-13 and GF-200.

Results and Discussion

Supramolecular formation of PEA-toly-UPy

The supramolecular chain extension of PEA-toly-UPy was confirmed by viscometric measurement. The coefficient viscosity of 40 mg/ml PEA-toly-UPy solution in chloroform is 21.7 ± 0.3 mPa·s at 28.0 °C. When an inhibitor of the supramolecular chain extension, Hexy-UPy, was added to this PEA-toly-UPy solution (molar ratio of UPy in the inhibitor to that in the polymer = 1/1), becames 2.94 ± 0.07 mPa·s at 26.5 °C. High viscosity of the PEA-toly-UPy solution indicates the formation of supramolecular polymers based on the quadruple hydrogen bonding between the UPy units. Supramolecular structure also gives clear effects on the film strength. PEA-hexy-UPy and PEA-toly-UPy give flexible free-standing films while PEA-diol forms only brittle film.

ATR-IR analysis of reference and PEA-UPys

UPy units have two tautomers, keto and enol forms. These tautomers can be distinguished by IR measurements[7,8].

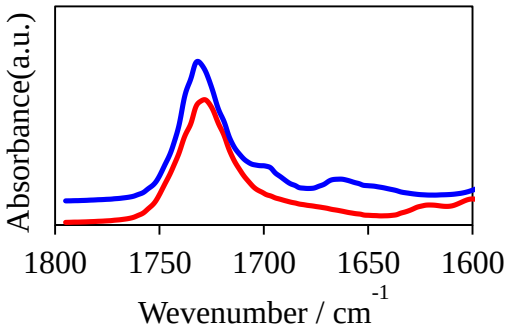

Figure 3-2-2 ATR-IR spectra of PEA-hexy-UPy (blue) and PEA-toly-UPy (red)

In the IR spectra, characteristic bands for the keto form appear at around 1660 and 1700 cm^{-1}, while those for the enol form appear peaks at around 1670 and 2600 cm^{-1}. In the case of PEA-toly-UPy at room temperature, the ATR-IR spectrum did not show any charactaristic peaks of keto forms (Fig.3-2-2), indicating that the UPy units in PEA-toly-UPy formed enol tautomers in the solid state. On the other hand, the spectrum of PEA-hexy-UPy has peaks at 1660 and 1700 cm^{-1} which are characteristic to the keto tautomers.

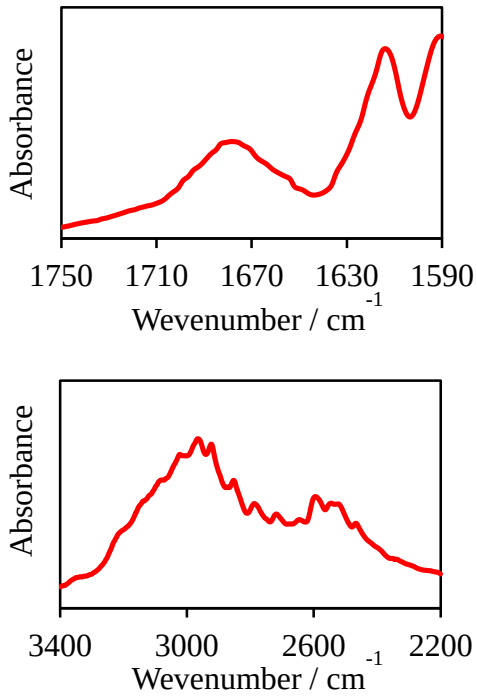

Figure 3-2-3 ATR-IR spectra of o-toly-UPy

As structural analogues of the end units of PEA-toly-UPy, o-toly-UPy was prepared. Peaks at 1670 and 2600 cm^{-1} appeared in an ATR-IR spectrum of o-toly-UPy, indicated that m-toly-UPy forms a enol tautomer. These results are the same as polymers.

It is known that UPy with electron-donating groups at the C6 position of the pyrimidinone ring form enol tautomers.[8] In this case, UPy of PEA-toly-UPy and o-toly-UPy have methyl groups at the position, which regularly form keto tautomers like PEA-hexy-UPy and p-toly-UPy. Therefore formation of enol tautomers in PEA-toly-UPy and o-toly-UPy would be induced from tolylene units.

Viscoelastic character of PEA-toly-UPy

Dynamic mechanical analysis was performed on PEA-toly-UPy. As shown in Figure 3-2-4, PEA-toly-UPy shows glass transition at -33 °C. The storage modulus at the rubber plateau is at 4×10^6 Pa, which gradually decreases above room temperature and intersects with the loss modulus at 49 °C. This results from melting of PEA. These results indicate that PEA-toly-UPy is at the rubber plateau.

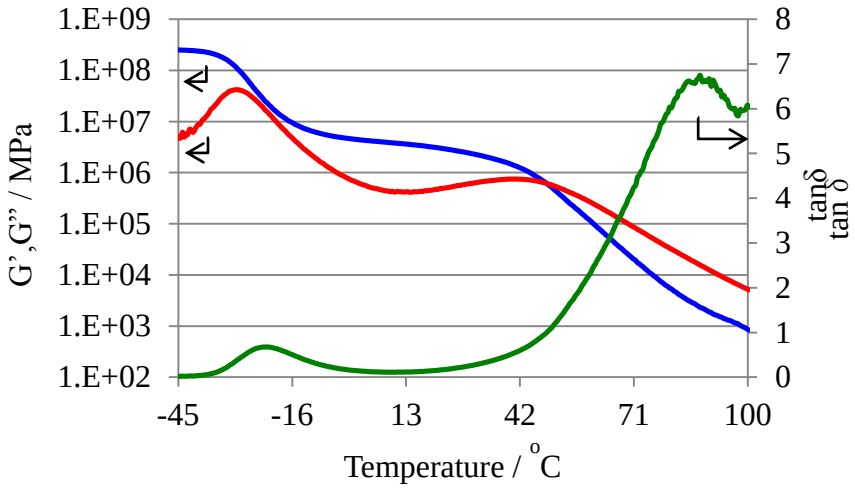

Figure 3-2-4 Visco elastic behavior of PEA-toly-UPy; storage module(blue, G'), loss module(red, G'') and tanδ(green)

Thermal properties of PEA-UPys

The progress of crystallization in PEA-diol and PEA-UPys was analyzed through the time course measurement of the enthalpy of fusion by DSC (Table 3-2-1).

Table 3-2-1. Progress of crystallization in PEA-diol and PEA-UPys

Polymer	Crystallization period[(a)]	T_m / °C	ΔH_f /Jg^{-1}	Degree of crystallinity[(b)] / %
PEA-diol	40 mins[(c)]	48	60	47[(c)]
PEA-hexy-UPy	1 day	42	22	18
PEA-hexy-UPy	2 days	42	44	35
PEA-hexy-UPy	1 week	41	44	35
PEA-toly-UPy	1 month	-[(d)]	≈ 0	≈ 0
PEA-toly-UPy	2 months	45	7.1	6
PEA-toly-UPy	5 months	44	18	14
PEA-toly-UPy	9 months	51	33	26
1/3PEA-toly-UPy / Hexy-Upy	2 months	44	35	27

(a): Crystallization periods at room temperature, (b): Estimated by dividing ΔH_f of the samples by the theoretical ΔH_f of 100 % crystalline PEA-diol (127 Jg^{-1}), (c): Crystallization reached equivalent, (d): No melting peak was observed.

After melting, PEA-diol took less than 40 mins to reach its equilibrium crystallinity (47%) when it isothermally crystalizes at 25 ^{o}C, while PEA-hexy-UPy required 2 days to reach the equilibrium (35%). The crystallization of PEA-toly-UPy proceeded on the year time scale. It is apparent that the terminal UPy moieties make the crystallization of PEA slower. When Hexy-UPy was added to PEA-toly-UPy (molar ratio of UPy in the inhibitor to UPy in the polymer = 3/1), the crystallization of PEA was accelerated. The degree of crystallinity reached 27% in two months. These results represent that the polymer chain extension by hydrogen bonding of UPy units makes the crystallization of PEA-UPys slower and that the bulky tolylene unit between PEA and UPy further reduces the crystallization rate.

ATR-IR analysis of cut surfaces

Figure 3-2-5 shows a part of the ATR-IR spectra of PEA-toly-UPy and PEA-hexy-UPy measured at the original uncut surface, the freshly-cut surface, the surface made by cut 2 days ago and the melt surface.

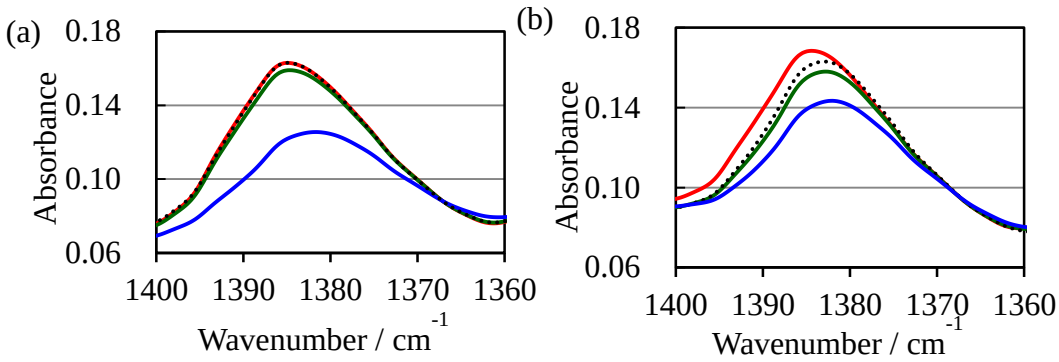

Figure 3-2-5 ATR-IR spectra of cut surfaces and melt surfaces; uncut surface(red line), cut surface(green line), cut surface after 2 days(dash line) and melt surface (blue line).(a)PEA-hexy-UPy, (b) PEA-toly-UPy.

The peak at 1385cm^{-1} (the asymmetrical wagging mode of CH_2) is sensitive to the crystallinity of PEA.[9] The comparison of the spectra measured at the original uncut surface and the melt surface shows that the crystalline phase gives a larger peak at higher wavenumber than the amorphous phase. For both PEA-toly-UPy and PEA-hexy-UPy, the cut surface gives a smaller peak at lower wavenumber than the original surface, indicating that the crystalline phase at the cut front is melted by the frictional heat created by cut. When the cut sample was kept at room temperature for 2 days, the crystallinity at the cut surface of PEA-Hex-UPy returned to the same level as the original surface, while the cut surface of PEA-toly-UPy still keeps lower crystallinity. As shown in Table 3-2-1, the crystallization of PEA-toly-UPy is extremely slow, which allows to maintain the low crystallinity at the cut surfaces for a long period.

Mechanical properties of PEA-UPys

Poly-hexy-UPy can form relatively high molecular weight chains via hydrogen bonding between UPy units. PEA-hexy-UPy give flexible free-standing films, however the films are too weak to perform tensile tests.

On the other hand, PEA-toly-UPy are able to be measured by tensile tests. Mechanical properties of PEA-toly-UPy(M_n^{NMR} = 5700, terminal modification rate of 82%, degree of crystallinity 1.2%) are as follows; young modulus = 1.7 ± 0.2 MPa; stress at yield = 0.60 ± 0.01 MPa; elongation at break = 1292 ± 205 %. Additionally, higher crystalized PEA-toly-UPy(M_n^{NMR} = 5900, terminal modification rate of 74%, degree of crystallinity 20%) becomes harder with young modulus = 38 ± 13 MPa; stress at yield = 3.2 ± 0.5 MPa; elongation at break = 22 ± 8 %.

Mending ability of PEA-hexy-UPy

Sample specimans of PEA-hexy-UPy (degree of crystallinity was 35 %) were cut by a knife into separated pieces, which were brought into contact and kept at room temperature without any external stress. After 2 days, the cut pieces of PEA-hexy-UPy were still separated, indicating that this polymer did not have mending ability at room temperature.

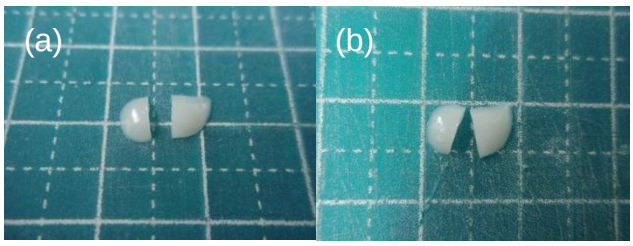

Figure 3-2-6 Mending properties of PEA-hexy-UPy: (a) freshly cut specimen of PEA-hexy-UPy; (b) the same specimen after mending for 2 days at room temperature

On the other hand, when the mending treatment performed at 60 ^{o}C, separated samples were joined in 10 min. The boundary line between cut surfaces disappeared after crystallization at room temperature and the cut samples perfectly joined(Figure 3-2-7). Therefore, PEA-hexy-UPy could be mended at melt state.

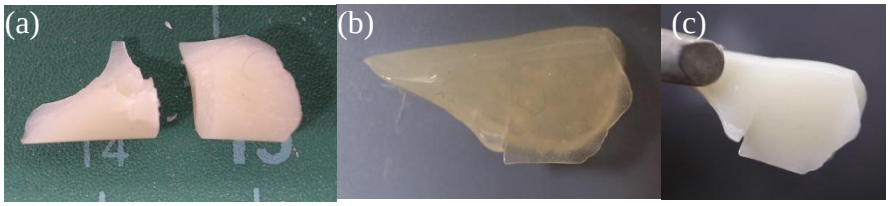

Figure 3-2-7 Mending properties of PEA-hexy-UPy at 60 ^{o}C: (a) freshly cut specimen of PEA-hexy-UPy, (b) the same specimen after mending for 10 min at 60 ^{o}C, (c) crystalizing sample after mending.

Behavior of PEA-hexy-UPy in mending procedures is linked to rate of crystallization(Table3-2-1) and low crystallinity at the cut surface (Figure 3-2-5).

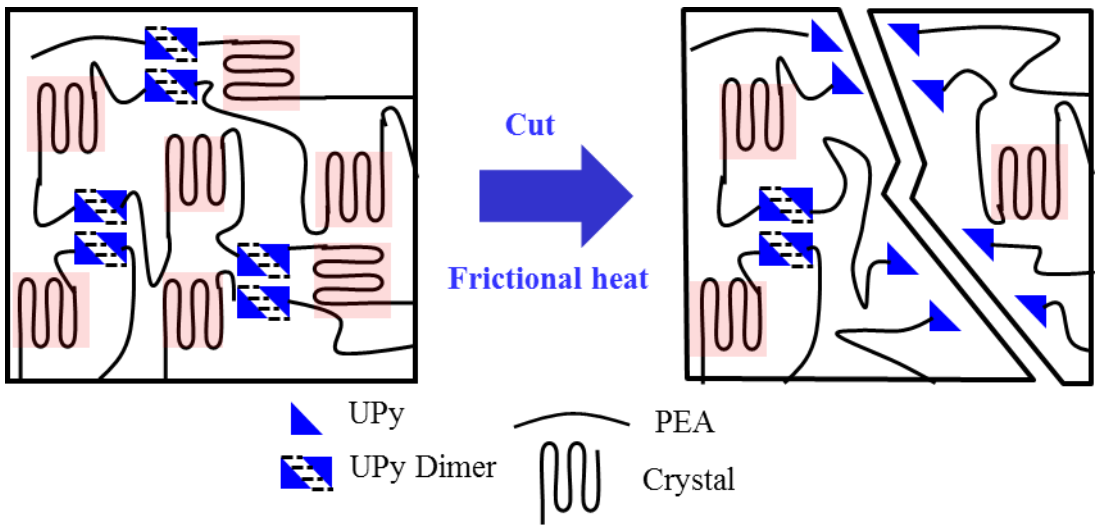

Figure 3-2-8 PEA-UPys after cut in molecular level.

Cutting of a bulk sample of PEA-UPys causes the cleavage of hydrogen bonds between UPy units at the cut front, which makes a number of free UPy units at the cut surfaces. At the same time, the frictional heat generated by cutting melts the crystals at the cut front to reduce the crystallinity at the cut surface(Figure 3-2-5). In

the case of PEA-hexy-UPy, fast crystallization inhibits the rejoining of the cut surfaces though a number of free UPy units might be generated by cutting at the cut front.

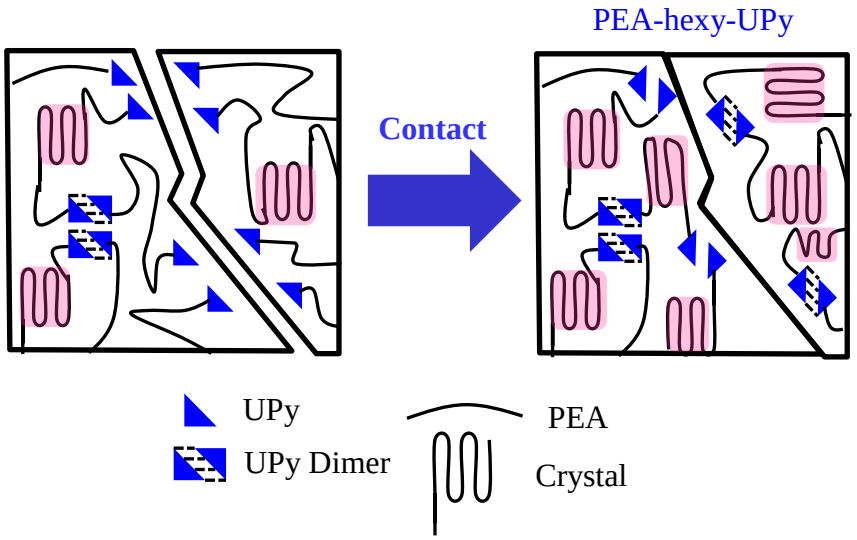

Figure 3-2-9 PEA-hexy-UPy after contact for 2 days at r.t. in molecular level

On the other hand, PEA-hexy-UPy mended by heat shock. Heating above melting temperature of PEA-hexy-UPy raised molecular mobility at cut surfaces and degree of crystallinity decreased more than that of cut samples at cut surfaces, therefore formation of UPy dimers from free UPy units and entanglement of polymers occurred to mend.

Mending ability of PEA-toly-UPy with low crystallinity

A sheet of PEA-toly-UPy, which did not crystalize, was cut into two pieces, and these cutting surfaces were immidiately contacted. After 5 min at room temperature, new combining portions generated between cut surfaces as shown in Figure 3-2-10. This shows that PEA-toly-UPy without crystallization has quick mending ability.

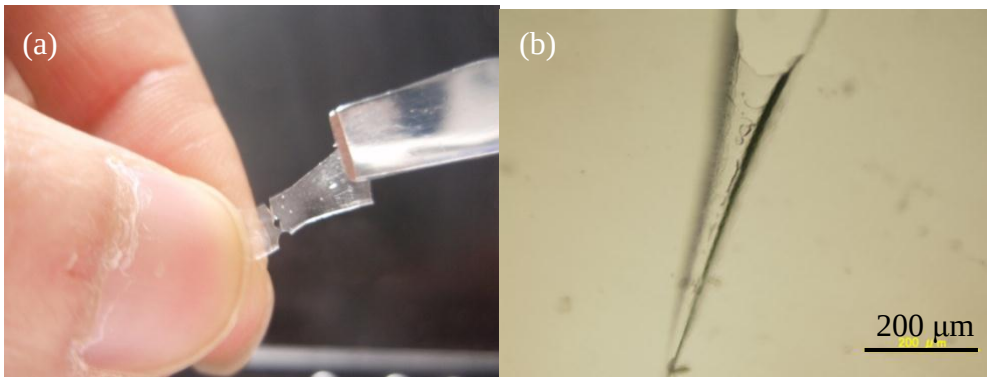

Figure 3-2-10 Mending properties of an amorphase PEA-toly-UPy sample: (a) a pulled sample after the cut surfaces were kept into contacted for 5 min at room temperature; (b) an optical microscopic image between cuting surfaces.

Recovery rates were calculated from tensile tests of original and mended PEA-toly-UPy. The recovery rates can be caluculated quantitatively based on the following equations;

$$R = \frac{X_{mended}}{X_{original}}$$

; X is value of mechanical properties such as maximum stress or elongation at break.

Samples for mending experiments were prepared by cast from chloroform (degree of crystallinity:0.88 %). Samples were cut into two pieces and kept into contact for 2 days at room temperature(Figure 3-2-11). After 2 days, tensile tests were performed.

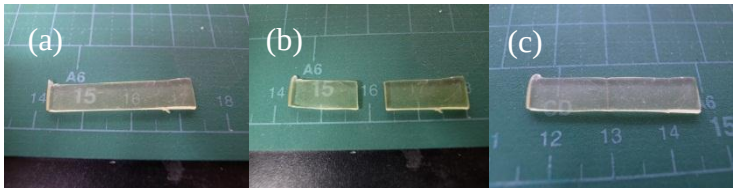

Figure 3-2-11 Samples of PEA-toly-UPy for tensile tests: (a)a sample before cut; (b) a cut sample; (c)a contacted sample.

The results of tensile test were shown in Figure 3-2-12. The mended samples could be performed to tensile tests and the results of mended samples were similar to those of original. However mended samples elonged less than originals and broke at cut positions.

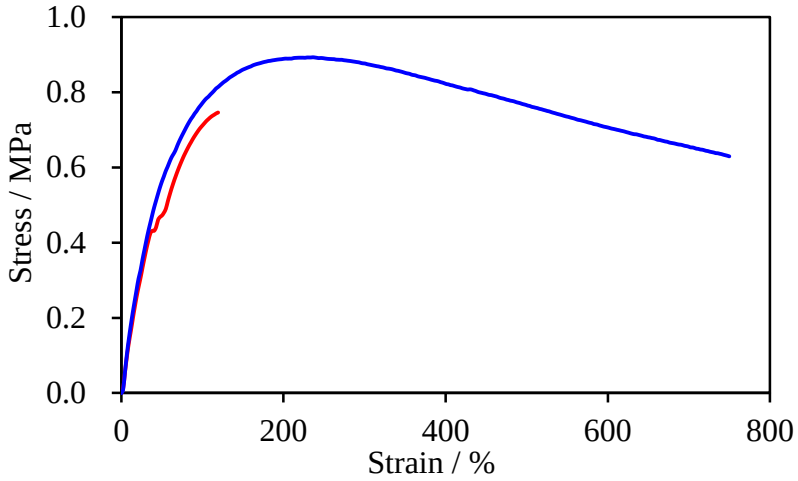

Figure 3-2-12 Tensile tests of original(blue) and mended(red) PEA-toly-UPy

Table3-2-2 showes the mechanical properties and recovery rates. The recovery rate of maximum stress were 85 % and that of elongation at break was 14 %. Recovery was well in elastic deformation region. In the case of mending materials consisting

of telechelic polymers, several days or one week are necessary for mend duo to low density of dynamic bonding units.[5,10] The longer samples were kept under contact, the more recovery rate increased. In this case,
2 days may be a little short and longer span for mand will give better recovery rate.

Table 3-2-2. Mechanical properties and recovery rates of PEA-toly-UPy

Sample	Young modulus / MPa	Maximum stress / MPa	Elongation at break / %	Recovery rate R / %	
				Maximum stress	Elongation at break
Original	1.4 ± 0.06	0.87 ± 0.04	785 ± 260	-	-
Mended	1.2 ± 0.39	0.73 ± 0.05	112 ± 12	85	14

On the other hand, the cut surfaces which were kept separated at room temperature for 2 days lost mending ability. Even if they were contacted with external force, they did not show any sign of mend. Immidiate contact after cut was neccesary for mend. Additionally, the mending property of PEA-toly-UPy has surface selectivity. The surfaces of an original uncut sample are not adhesive. They stick to neither another original surface nor a freshly-cut surface. Mending can occur only between the freshly-cut surfaces of PEA-toly-UPy.

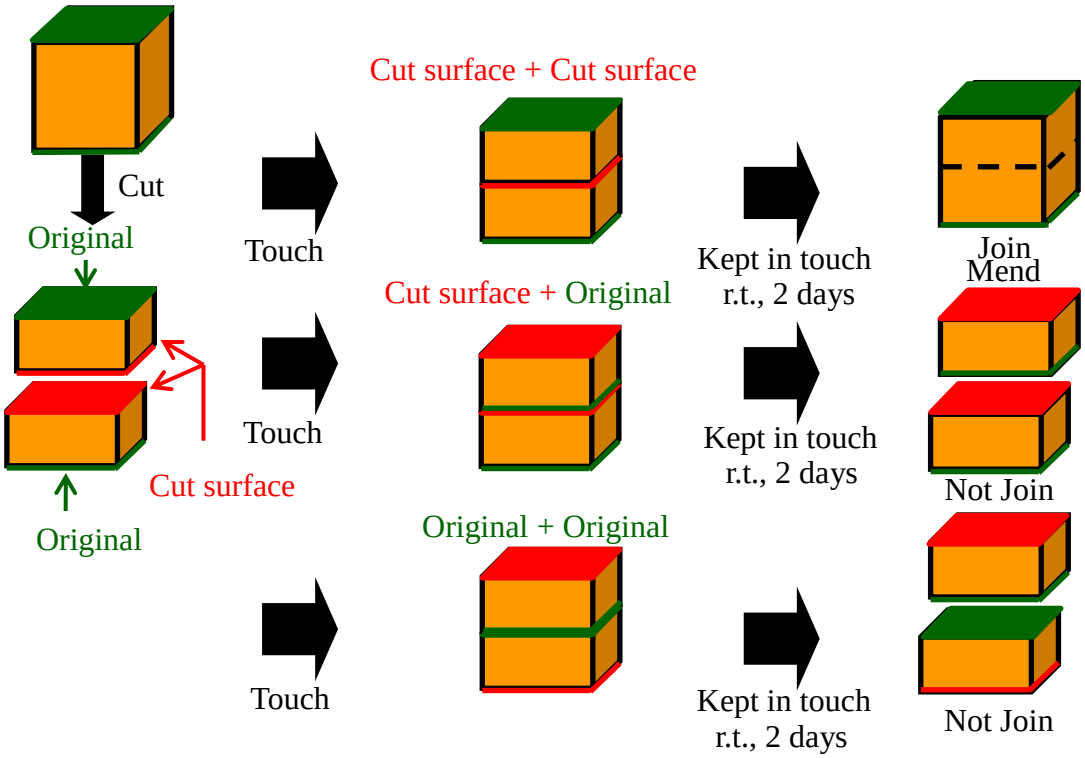

Figure 3-2-13 Surface selective mending properties of PEA-toly-UPy

Mending ability of crystalized PEA-toly-UPy

The mending experiments were also peformed to sample specimens of PEA-toly-UPy whose degree of crystallinity reaches 14 %. Sample specimans were cut by a knife into separated pieces, which were brought into contact and kept at room temperature without any external stress.

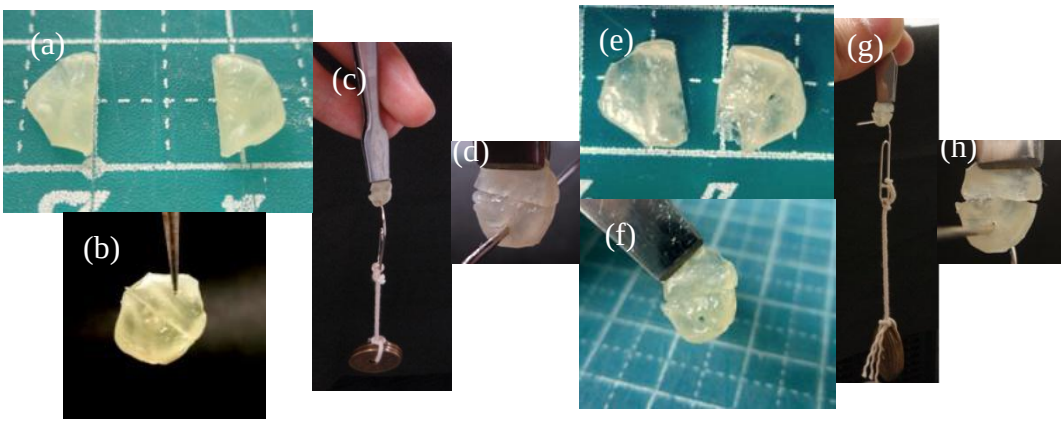

Figure 3-2-14 Mending properties of PEA-toly-UPy (degree of crystallinity:14 %): (a) a freshly cut specimen of PEA-toly-UPy; (b) the same specimen after mending for 2 days at room temperature; (c) A sample specimen after the first mending experiment can sustain a hung weight; (d) enlarged view of (c); (e,f) the same process was repeated on the same specimen at the same position; (g,h) the same specimen after the second mending experiment at the same position can sustain the same weight.

After 2 days, PEA-Toly-UPy was mended enough to suspend some weights(section area 12 mm^2, weight 12 g). A visual demonstration of mend for PEA-toly-UPy is given in Figure 3-2-14(a)-(d). Further, these cut and mend process is repeatable(Fig. 3-2-14(e)-(f)). The sample after mending was cut again at the same position and stayed on contact for 2 days at room temperature. The sample after repeated mending could lift the same weight as the first experiment. Therefore, PEA-toly-UPy had repeatable mending ability at room temperature.

Additionally, crystallized PEA-toly-UPy also has surface selective mending ability at room temperature, described in Figure 3-2-13.

Higher crystalized PEA-toly-UPy(degree of crystallinity:26 %) also had mending

ability at room temperature(Fig.3-2-15).

Figure 3-2-15 Mending properties of PEA-toly-UPy (degree of crystallinity:26 %): (a) a freshly cut specimen of PEA-Toly-UPy; (b) the same specimen after mending for 2 days at room temperature; (c) A sample specimen after the mending experiment can sustain a hung weight; (d) enlarged view of (c).

On the other hand, the same procedures were peformed to the 1/3 mixture of PEA-toly-UPy / Hexy-UPy. The results are shown in Figure 3-2-16. After 2 days, the cut pieces of mixture were still separated, indicating that the mixture did not have mending ability at room tempetature.

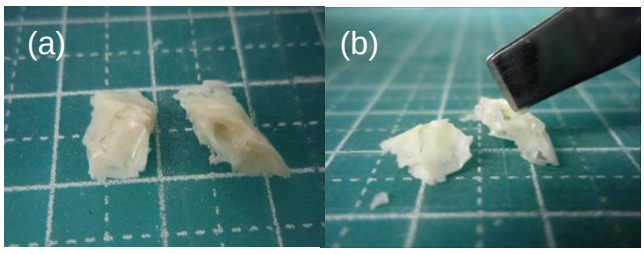

Figure 3-2-16 mending properties of the 1/3 mixture of PEA-toly-UPy / Hexy-Upy: (a) freshly cut specimen of the mixture; (b) the same specimen after mending for 2 days at room temperature

Mending behavior of PEA-toly-UPy is also linked to this low crystallinity at the cut surface and the reversibility of hydrogen bonding (Figure 3-2-8). The cleavage of hydrogen bonds between UPy units and reducing the crystallinity at the cut surfaces also occur in PEA-toly-UPy by cut.

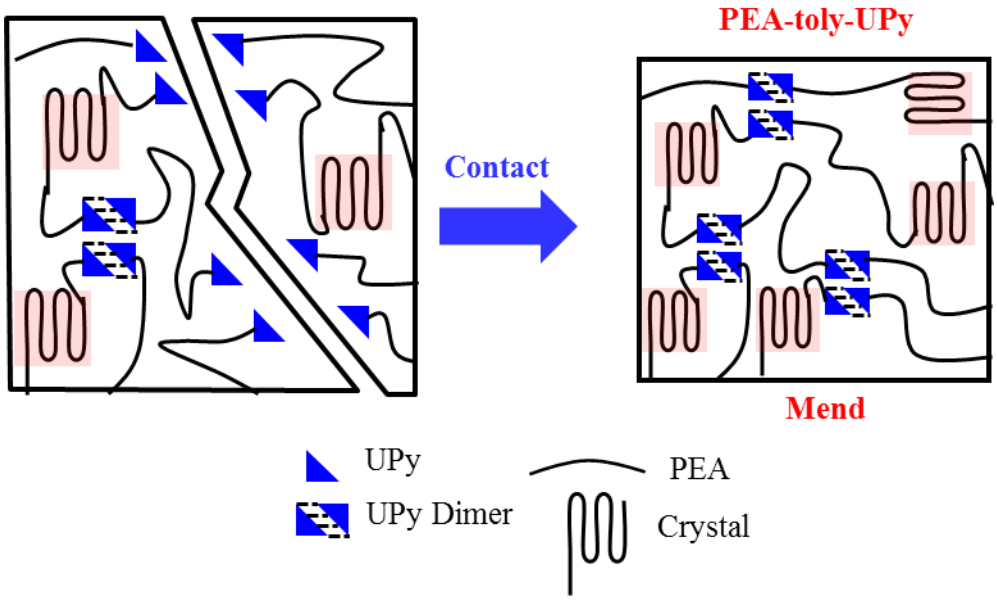

Figure 3-2-17 PEA-toly-UPy after contact for 2 days at r.t. in molecular level

Because of the extremely slow crystallization of PEA-toly-UPy, the molecular mobility near the cut surface is maintained for a long period even at room temperature. If the cut surfaces are in contact with each other, hydrogen bonds can be reformed between the free UPy units to rejoin the cut surfaces. Since the frictional heat melts only the crystals at the cut front, the bulk crystallinity of PEA-toly-UPy is kept throughout the mending process. Therefore, except for the direct damage by cutting, no negative effects are introduced by this mending mechanism.

If sample after mend was cut at the same position, reduction in degree of crystallinity and cleavage of hydrogen bonds occurred again. These were the same as the first cut and contact of both cut surfaces induced mending mechanism to mend. Therefore, mend of PEA-toly-UPy can repeat at room temperature. At uncut surfaces, degree of crystallinity is high, which means low molecular mobility, and free UPy units do not exist. Therefore, uncut surfaces did not join with any surfaces even if freshly cut surfaces. Additionally, cut samples kept at room temperature for 2 days without contact of cut surfaces did not mend. This is because free UPy units form dimers in cut surfaces during 2 days and this leads to losing mendability. After 2 days, conditions of cut surfaces are similar to those of uncut surfaces and they do not join with any surfaces.

The 1/3 mixture of PEA-toly-UPy / Hexy-UPy also did not mend at room temperature. The cleavage of hydrogen bonds between UPy units and reducing the crystallinity at the cut surfaces may occur by cutting. Faster crystalline rate of the mixture, shown in Table 3-2-1, results in immidiate decrease of molecular mobility at cut surfaces. is faster, therefore reformation of UPy dimer do not occur between cut surfaces. Additionally, Hexy-UPy inhibited chain extension by UPy units. This lead to less cleavage of hydrogen bonds between UPy units because this cleavage result from tension of polymer chains by external stress. These changes from PEA-toly-UPy resulted in lose of mending ability.

Conclusion

The author proposes a novel approach to obtain crystalline polymers with mending ability at room temperature. To a target crystalline polymer, bulky units are introduced to reduce the crystallization rate. Dynamic bonds are also combined to introduce the reversibility to the polymer. In this crystalline polymer, cutting samples invokes dissociation of dynamic bonds and reduction of crystallinity at the cut surfaces. Due to the slow crystallization, high molecular mobility at the cut surfaces is maintained for a long period, which allows the reformation of dynamic bonds between the cut surfaces to repair. Because of the reversibility of the dynamic bond, this mending mechanism works repeatedly at the same position.

3-3 Elastic materials with mending ability at room temperature

Introduction

In Chapter 3-3, for improvement of mechanical properties of the mendable polymer described in Chapter 3-2, new materials were obtained as below. Another crystalline polymer, poly(ethylene succinate)[PES], was inserted into the center of tolylene and UPy terminated PEA to form ABA type block polymer. Crystallization of PES is fast and not inhibited by UPy and tolylene units due to far distance between UPy and PES, therefore PES is easy to crystallize. Additionally, PEA and PES are immiscible. Therefore, crystalline phase of PES and micro phase separation lead to physical crosslinks in ABA block polymers and these make mendable polymers tougher.

Experimental section

Synthesis of poly(ethylene succinate) diol [PES-diol].

PES-diol was synthesized by two-step polycondensation reactions as follows. A mixture of succinic acid(8.992 g, 76.2 mmol) and ethylene glycol(5.196 g, 83.8 mmol) with the molar ratio of succinic acid / ethylene glycol = 1/1.1 was melted and stirred at 200 °C for 2 h with exclusion of water. The reaction mixture was stirred at 200 °C under a reduced pressure (<2 mmHg) for 4 h. After cooling to room temperature, the product was dissolved in chloroform, precipitated with methanol at 0 ^{o}C and dried under vacuum. The yield was 9.698 g. ^{1}H NMR: [$CDCl_3$], δ/ppm 2.68 (br, CH_2), 3.82 (t, CH_2), 4.24 (t, CH_2), 4.30 (br, CH_2), M_n^{NMR} = 4700; M_n^{GPC} = 4000, M_w/M_n = 1.5.

Synthesis of PEA-PES-UPy.

Tolylene-2,4-diisocyanate-terminated poly(ethylene adipate) (10.533 g, 1.92 mmol,

M_n^{NMR} = 5500) and PES-diol(1.056 g, 0.224 mmol, M_n^{NMR} = 4700) were dissolved in dehydrated chloroform (60 ml) under N_2 and stirred at 50 ^oC for 2 days. 2-amino-4-hydroxy-6-methylpyrimidine (2.061 g, 16.2 mmol) was added to reaction solvent and stirred under reflux for 1 day. 50 ml of *N*,*N*-dimethylformamide was added to the mixture and then chloroform was removed from the mixture by evaporation. The product was obtained by filtration and precipitation with excess water at room temperature and dried under vacuum at 80 °C. The yield was 11.885 g. ^{1}H NMR: [$CDCl_3$], δ/ppm 1.65 (br, CH_2), 3-30 (s, CH_3), 3-36 (s, CH_3), 3-36 (br, CH_2), 2.64(br, CH_2), 4.0-4.50 (m, CH_2), 5.82 (s, CH), 6.71 (br, NH), 7.13–8.00 (m, aromatic, overlapping chloroform peaks), 11.79 (br, CH), 13-36 (br, NH), 12.99 (br, NH).

PEA-PES-UPy(II) was synthesized on the same procedure. The weight ratio of PEA-diisocyanate and PES-diol was 5:1. Obtained mixture PEA-PES-UPy contained PEA-toly-UPy and PEA-PES PEA block polymer with UPy units. Main component was PEA-toly-UPy.

Two kinds of PEA-PES-UPy with different content rates of PES were synthesized.

PEA-PES-UPy(I) contained smaller amount of PEA. The monomer ratio of PEA and PES, calculated from ^{1}H-NMR spectra, was 7.8:1. PEA-PES-UPy(II) had more PES segments, the monomer ratio was 4.8:1.

Scheme 3-3-1 synthesis of PEA-PES-UPy

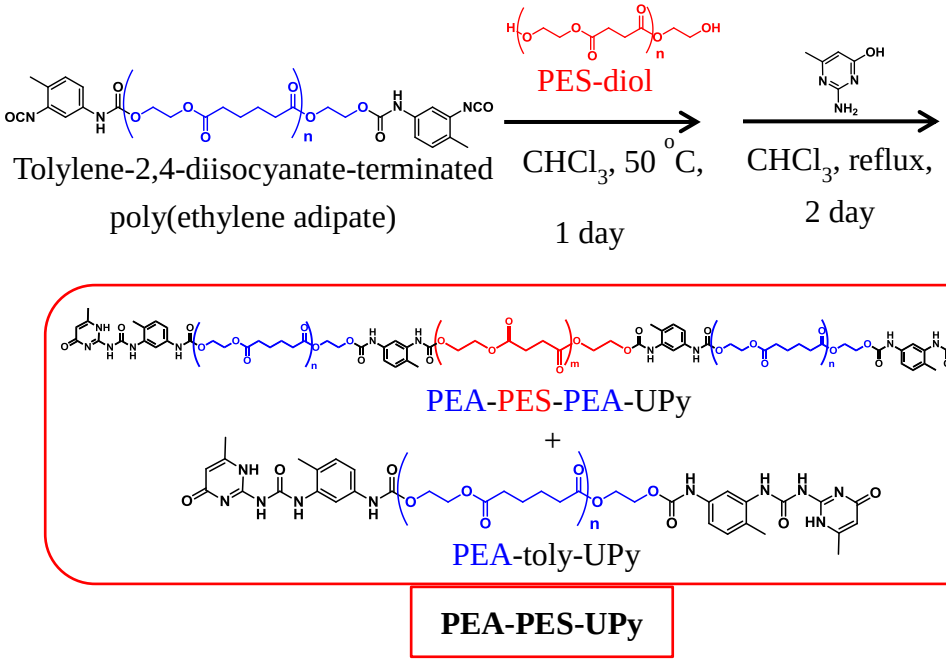

Analytical Procedures.

^{1}H NMR spectroscopy was performed using JEOL JNM-ECS400 NMR SYSTEM. The monomer ratio of PEA and PES, calculated from ^{1}H-NMR spectra by comparing the peak areas of main chain of PEA and PES.

Gel permeation chromatography (GPC) was carried out using Tosoh HLC 8220 GPC system equipped with TSK-Gel GMH_{HR}-N columns (chloroform, 40 ^{o}C, 1 mg mL^{-1}). Polystyrene standards with low polydispersity were used to construct a calibration curve.

Atomic force microscopy(AFM) was carried out with Seiko Instruments Inc. Nano cute.

Differential scanning calorimetry (DSC) was carried out with Perkin-Elmer Pyris 1 at a heating rate of 10 ^{o}C/min under a N_2 atmosphere. Melting temperature, T_m, and heat of fusion, ΔH_f, was taken as the peak top and the area of the melting endotherm,

respectively. The crystallinity was calculated by dividing ΔH_f of the sample with theoretial ΔH_f value of PEA-diol and PES-diol with 100% crystallinity.

Mechanical properties of film samples were evaluated using a tensile testing machine, SHIMADZU EZ test, at a cross-head speed of 10 mm min^{-1} at room temperature. The dumbbell specimens of samples (with the center section 1.4 mm wide, 7.0 mm long and 0.5 mm thick) were used. Values of Young modulus, stress at yield, and elongation at break were averaged over the data of at least three specimens. Recovery rates were calculated from tensile tests at a cross-head speed of 10 mm min^{-1} at room temperature. The rectangle specimens of samples (with the center section 4 - 6 mm wide, 7.0 mm long and 0.4 mm thick) were used.

Results and Discussion

Immiscibility of PEA and PES

Immiscibility of PEA and PES was checked. PEA-toly-UPy and PEA-diol were mixed in the same weight. Glass transition temperature(T_g) were checked by DSC after melt and immediate quenched to -50 ^oC. The 1/1 mixture of PEA-toly-UPy and PES-diol had two T_g at -30 and -15 ^oC during heating scan and the former came from PEA and the latter was from PES, indicated that PEA and PES are immiscible.(Figure3-3-1)

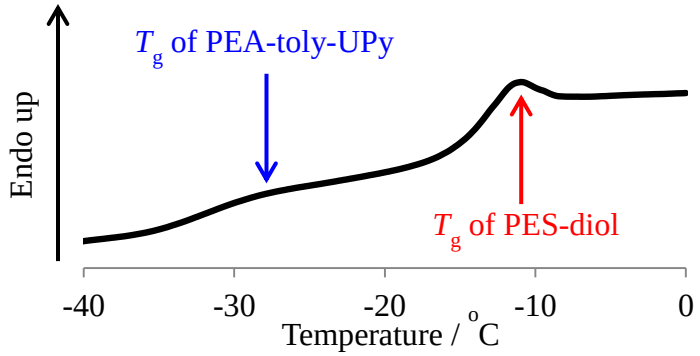

Figure 3-3-1 DSC curve of the 1/1 mixture of PEA-toly-UPy and PES diol during 2nd heating scan

Additionally, PEA-PES-UPy(I) was measured by AFM. Polymer films were prepared on glass plates by spin coasting from chloroform solution of the polymer.

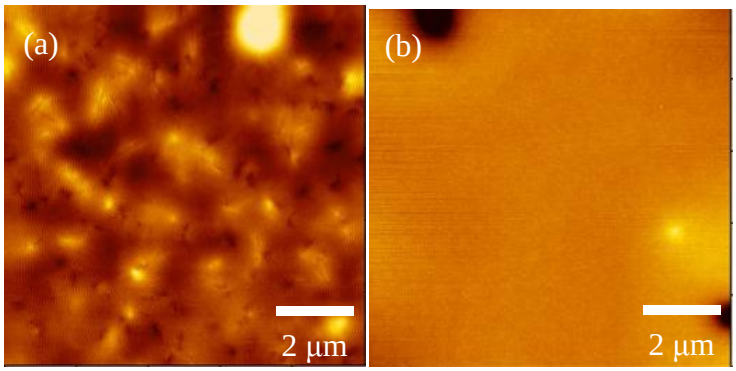

Figure 3-3-2 AFM height images; (a)PEA-PES-UPy, (b)PEA-toly-UPy

After 1day, height images were measured and micro size phase separation was confirmed(Figure3-3-2). In the case of PEA-toly-UPy, micro phase separation did not appear. Because of immiscibility of PEA and PES, PES separated from PEA .

Thermal properties of PEA-PES-UPy

The progress of crystallization in PEA-PES-UPy was analyzed through the time course measurement of the enthalpy of fusion by DSC.

Table 3-3-1 crystallization of PEA-PES-UPy(I)

Span / day	T_m (PEA) / ^oC	ΔH_f (PEA)[(a)] / Jg^{-1}	ΔH_f^{cal} (PEA)[(b)] / Jg^{-1}	Degree of crystallinity[(c)] / %	T_m (PES) / ^oC	ΔH_f (PES)[(d)] / Jg^{-1}	ΔH_f^{cal} (PES)[(e)] / Jg^{-1}	Degree of crystallinity[(f)] / %
1	-	-	-	-	95	4.3	44	29
57	46	16	17	14	96	4.1	43	28
112	46	29	32	25	95	4.1	42	28

(a): Heat quantity / sample weight, (b): Heat quantity / PEA weight, c;estimated by dividing ΔH_f of the samples by the theoretical ΔH_f of 100 % crystalline PEA-diol (127 Jg^{-1}), (d): Heat quantity / PES weight, (e): Heat quantity / PEA weight, (f): Estimated by dividing ΔH_f of the samples by the theoretical ΔH_f of 100 % crystalline PEA-diol (152 Jg^{-1}).

Table 3-3-2 crystallization of PEA-PES-UPy(II)

Span / day	T_m (PEA) / °C	ΔH_f (PEA)[a] / Jg^{-1}	ΔH_f^{cal} (PEA)[b] / Jg^{-1}	Degree of crystallinity[(c)] / %	T_m (PES) / °C	ΔH_f (PES)[(d)] / Jg^{-1}	ΔH_f^{cal} (PES)[(e)] / Jg^{-1}	Degree of crystallinity[(f)] / %
1	-	-	-	-	92	5.5	37	24
83	49	18	21	16	92	5.6	37	25
132	51	28	33	26	95	5.5	37	24

(a): Heat quantity / sample weight, (b): Heat quantity / PEA weight, c;estimated by dividing ΔH_f of the samples by the theoretical ΔH_f of 100 % crystalline PEA-diol (127 Jg^{-1}), (d): Heat quantity / PES weight, (e): Heat quantity / PEA weight, (f): Estimated by dividing ΔH_f of the samples by the theoretical ΔH_f of 100 % crystalline PEA-diol (152 Jg^{-1}).

After melting at 120 °C, a melting peak of PEA did not appear for 1 day at room temperature in both PEA-PES-UPy during a heating scan while a peak from PES appeared at 95 °C. Crystallization of PEA gradually proceeded at r.t. and a melting peak was appeared after 57 days in the case of PEA-PES-UPy(I). Table 1 showes that the values of ΔH_f^{cal} and degree of crystallinity, which caluculated from ΔH_f and monomer ratio of PEA and PES, were constant after 1 day from melt, indicating that crystallization of PES reached equivalent in 1 day, and that of PEA was slow. Compared PEA-PES-UPy(II) with PEA-PES-UPy(I), degree of crystallinity of PES was almost the same.

Mechanical properties of PEA-PES-UPys and PEA-toly-UPY

Figure3-3-4 and Table3-3-3 shows the results of tensile test of PEA-toly-UPy and PEA-PES-UPys. Each samples had different mechanical properties.

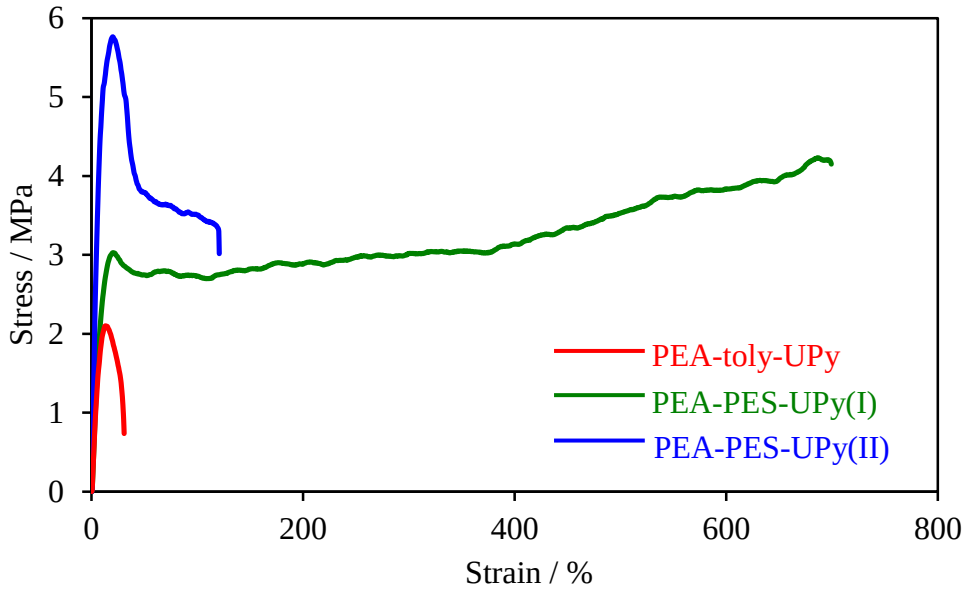

Figure 3-3-4 Mechanical properties of PEA-PES-UPys and PEA-toly-UPy

Table3-3-3 Mechanical properties of PEA-PES-UPys and PEA-toly-UPy

Sample	Stress at yield / MPa	Young modulus / MPa	Elongation at break / %
PEA-PES-UPy(I)[(a)]	3-3 ± 0.2	34 ± 3	665 ± 63
PEA-PES-UPy(II)[(b)]	5.4 ± 0.4	59 ± 6	126 ± 34
PEA-toly-UPy[(c)]	2.2 ± 0.5	38 ± 13	22 ± 8

(a): Degree of crystallinity(PEA 20 %), (PES 26 %), (b): Degree of crystallinity (PEA 18%), (PES 24 %), (c): Degree of crystallinity(PEA 20 %).

Crystallized PEA-toly-UPy was harder and less elastic than low crystallized one, shown in Fig.3-1-12. Because the crystalline phase gives hardness and the soft amorphous phase gives toughness to materials, polymers with higher crystallinity become not only harder but also less elastic. While stress at yield and Young module of PEA-PES-UPy(I) were almost the same as PEA-toly-UPy, elongation at break was fairly larger. PEA-PES-UPy(I) was elastic because PES segments, which crystallized and separated from PEA segments, acted as physical crosslinking points. On the other hand, PEA-PES-UPy(II) had larger stress at yield, young module and smaller elongation at break than those of PEA-PES-UPy(I) in spite of similar degree of crystallinity. This is because PEA-PES-UPy(II) had more physical crosslinking points, PES segments, than PEA-PES-UPy(I) and these crosslinks make the polymer harder.

Mending experiment of PEA-PES-UPys

Sample specimans of PEA-PES-UPy(I) (degree of crystallinity:PEA 1.1 %, PES 29 %) for mending experiments were cut by a knife into separated pieces, which were brought into contact and kept at room temperature without any external stress. After two days, the cut pieces of PEA-PES-UPy(I) was mended enough to suspend some weights. A visual demonstration of the mending process for PEA-PES-UPy(I) is given in Figure3-3-5. The mending property of PEA-PES-UPy(I) also has surface selectivity and repeatable mending ability like PEA-toly-UPy (Figure3-3-5(e)-(h)).

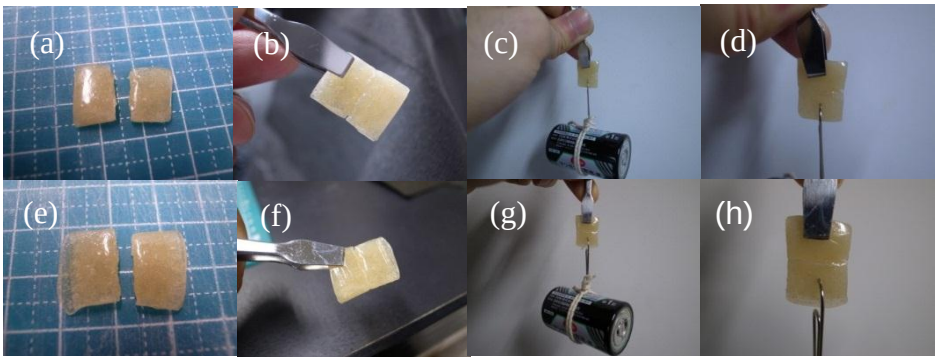

Figure 3-3-5 mending properties of PEA-PES-UPy(I): (a) freshly cut specimen (b) the same specimen after mending for two days at room temperature; (c) A sample specimen after the first self-mending experiment can sustain a hung weight(section area 26 mm^2, weight 110 g); (d) enlarged view of (c); (e,f) the same process was repeated on the same specimen at the same position; (g,h) The same specimen after the second self-mending experiment at the same position can sustain the same weight.

Recovery rates were calculated from tensile tests of original and mended PEA-PES-UPy(I). The samples were prepared by compression-molding of the solvent-cast films between two Teflon sheets with an aluminum spacer (0.5 mm thickness using a hot press (Imoto Co., Japan) at 120 ^oC for 20 min under a pressure of 6 MPa and following crystallization at room temperature (degree of crystallinity:PEA 1.5 %, PES 27 %). Samples were deeply cut and kept into contact for two days at room temperature(Figure 3-3-6). After two days, tensile tests were performed.

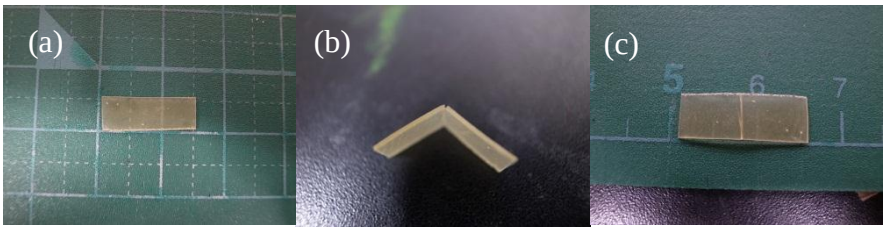

Figure 3-3-6 Samples of PEA-PES-UPy for tensile tests: (a)a sample before cut; (b) a deeply cut sample; (c)a contacted sample.

Like PEA-toly-UPy in Chapter3-1, the mended samples could be performed to tensile tests and the results of mended samples were similar to those of original shown in Figure 3-3-7. However these also elonged less than originals and broke at cut positions.

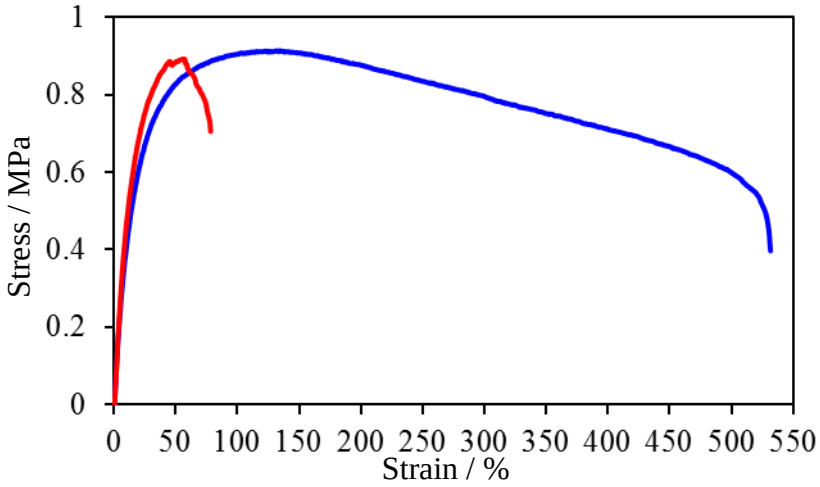

Figure 3-3-7 Tensile tests of original(blue) and mended(red) PEA-toly-UPy

Table3-3-3 showes the mechanical properties and recovery rates. The recovery rate of maximum stress were 77 % and that of elongation at break was 14 %. These

results show that PEA-PES-UPy has similar mending properties at room temperature.

Table 3-3-3. Mechanical properties and recovery rates of PEA-PES-UPy

Sample	Young modulus / MPa	Maximum stress / MPa	Elongation at break / %	Recovery rate R / %	
				Maximum stress	Elongation at break
Original	4.1 ± 0.06	0.93 ± 0.02	526 ± 89	-	-
mended	4.4 ± 0.70	0.72 ± 0.18	75 ± 7	77	14

On the other hand, the same mending experiment was performed to sample specimens of PEA-PES-UPy(I) (degree of crystallinity:PEA 9 %, PES 22 %). Althoug crystallinity of PEA was higher, this sample mended after two days at room temperature(Figure3-3-8(a)-(d)). Therefore, PEA-PES-UPy(I) have mending ability at room temperature even if each constituent crystalizes.

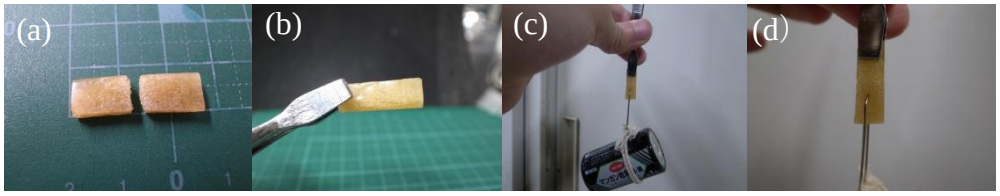

Figure 3-3-8 mending properties of PEA-PES-UPy(I): (a) freshly cut specimen (b) the same specimen after mending for two days at room temperature; (c) A sample specimen after the first self-mending experiment can sustain a hung weight(section area 25 mm^2, weight 110 g); (d) enlarged view of (c).

Mending mechanism of PEA-PES-UPy

Mending behavior of PEA-PES-UPy(I) is similar to that of PEA-toly-UPy.

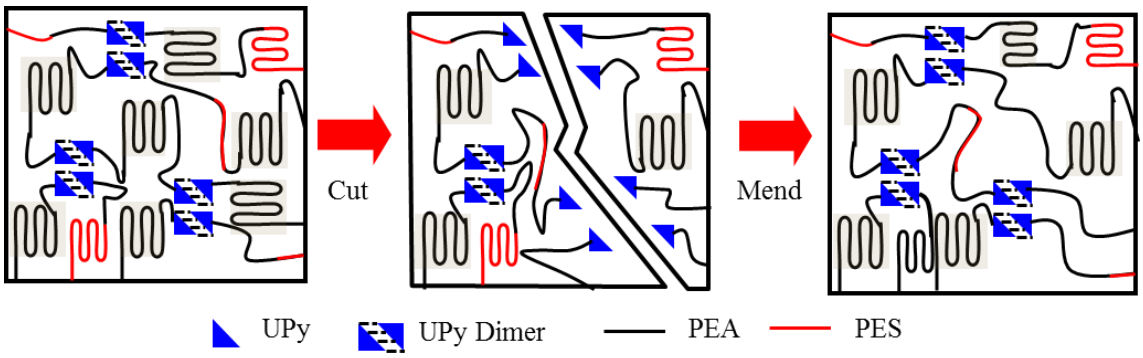

Figure 3-3-9 mending mechanism of PEA-PES-UPy

However, PEA-PES-UPy(I) has PES segments which crystalize fast. Sample of PEA-PES-UPy(I) caused low crystallinity at the cut surfaces and the cleavage of hydrogen bonds between UPy units. Although melting of PES crystal occured, PES immediately re-crystalized dut to fast crystallization of PES descrided above. Therefore PES crystal existed near cut surfaces. On the other hand, low crystallinity of PEA continued for a long period because PEA slowly crystalized in PEA-PES-UPy(I) like PEA-toly-UPy, shown in Table 3-3-1. PEA is linked to UPy units, which relates to mending mechanism. Low crystallinity of PEA induced high molecular mobility around UPy units, and free UPy units formed by cut re-dimerized between cut surfaces to mend. These processes for mend are the same as PEA-toly-UPy, therefore PEA-PES-UPy similaly has repeatable and surface selective mending ability at room temperature.

Conclusion

PEA-PES-UPy consisted by PEA-toly-UPy and ABA block polymers with PES segment at the center were synthesized. These were more elastic than PEA-toly-UPy because PES segments were crystallized and phase separated from PEA segments to work physical crosslinking points. PEA-PES-UPy having more PES segments became less elastic because of higher crosslinking densities. Additionally, PEA-PES-UPy also had repeatable mending ability at room temperature as PEA-toly-UPy.

3-4. Reference in Chapter3

[1]a) D. Y. Wu, S. Meure and D. Solomon, *Prog. Polym. Sci.*, **2008**,3-3**,** 479; b) E. B. Murphy and F. Wudl, *Prog. Polym. Sci.*, **2010**, *35*,3-33.

[2] (a) X. X. Chen, M. A. Dam, K. Ono, A. Mal, H. B. Shen, S. R. Nutt, K. Sheran and

F. Wudl, *Science*, **2003**, 3*95*, 1698, b) E. B. Murphy, E. Bolanos, C. Schaffner-Hamann, F. Wudl, S. R. Nutt and M. L. Auad, *Macromolecules*, **2008**, *41*, 5203.

[3](a)G. Deng, C. Tang, F. Li, H. Jiang and Y. Chen, *Macromolecules*, **2010**, *43*, 1191, (b)P. Cordier, F. Tournilhac, C. Soulie-Ziakovic and L. Leibler, *Nature*, **2008**, *451*, 977, (c)Q.Wang, J. L. Mynar, M. Yoshida, E. Lee, M. Lee, K. Okuro, K. Kinbara and T. Aida, *Nature*, **2010**, *463-339*.

[4](a)S. Burattini, H. M. Colquhoun, J. D. Fox, D. Friedmann, B. W. Greenland, P. J. F. Harris, W. Hayes, M. E. Mackay and S. J. Rowan, *Chem. Commun.*, **2009**, 6717, (b)B. Ghosh and M. W. Urban, *Science*, **2009**, *323*, 1458.

[5]N. Yoshie, M. Watanabe, H. Araki, K. Ishida, *Polym. Degrad. Stab.***, 2010**, *95*, 826.

[6]a) R. P. Sijbesma, F. H. Beijer, L. Brunsveld, B. J. B. Folmer, J. Hirschberg, R. F. M. Lange, J. K. L. Lowe and E. W. Meijer, *Science*, **1997**, *278*, 1601, b) B. J. B. Folmer, R. P. Sijbesma, R. M. Versteegen, J. A. J. van der Rijt and E. W. Meijer, *Adv. Mater.*, **2000**, *12*, 874, c) A. W. Bosman, R. P. Sijbesma, and E. W. Meijer, *Materials Today*, **2004**, 34.

[7] V. G. H. Lafitte, A. E. Aliev, H. C. Hailes, K. Bala and P. Golding, *J. Org. Chem.*, **2005**, *70*, 2701.

[8] (a)F. H. Beijer, R. P. Sijbesma, H. Kooijman, A. L. Spek, E. W. Meijer**,** *J. Am. Chem. Soc.* **1998,** *120*, 6761, (b) T. F. A. de Greef, G. B. W. L. Ligthart, M. Lutz, A. L.

Spek, E. W. Meijer, R. P. Sijbesma,*J. Am. Chem. Soc.*, **2008**, *130*, 5479.

[9] J. J. Yang, P. J. Pan, T. Dong and Y. Inoue, *Polymer*, **2010**, *51*, 807.

[10]N. Yoshie, S. Saitoh, N. Oya, , *Polymer*, **2011**, *52*, 6074.

Chapter 4.

Mechanical property tuning of semicrystalline network polymers by controlling rates of crystallization and crosslinking

Introduction

Network polymers are industrially important because they can be both glassy hard thermosets and soft elastomers depending on the crosslink density. They are widely used as structural materials, rubbers, adhesives,[1] and gels.[2] Network polymers with mending ability[3] and shape memory[4] are also developed. In semicrystalline network polymers, crosslinking and crystallization mutually affect each other.[5-7] Crosslinks lead less perfect crystalline packing, resulting in reduction of crystallinity and crystallite size, while the preformed crystals inhibit crosslink formation and affect the resultant network structure. This structural variation significantly influences the mechanical properties of network polymers. Therefore, control of crosslinking and crystallization is important to obtain desirable materials.

Network polymers crosslinked by dynamic bonds are attractive and have been applied to smart materials using their reversibility.[8] As a reversible crosslink, the Diels-Alder (DA) reaction of furan and maleimide is widely used.[9,10] The forward cycloaddition reaction progresses at mild temperature without byproducts while the reverse dissociation reaction (rDA reaction) occurs above 100 °C. As described in previous Chapter, Yoshie lab. also reported network polymers made by DA reaction of telechelic prepolymers having furan end groups and a tris-maleimide linker.[11-13] In these study, when semicrystalline polymers are selected as a main chain of the telechelic prepolymers, the network polymers exhibit two-way conversion between hard and soft properties(Figure4-1).[14-16]

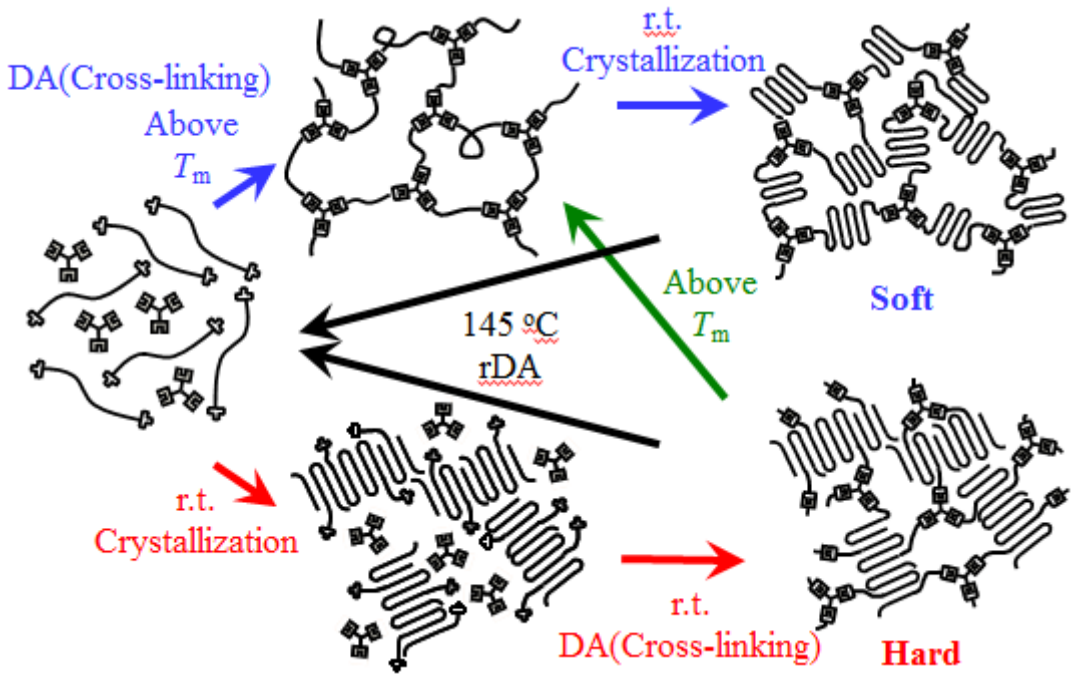

Figure 4-1. Schematic representation of two-way conversion between hard and soft mechanical properties induced by controlling the dynamics of melt/crystallization and crosslinking/decrosslinking.

The network polymers crosslinked in the presence of crystalline phase are relatively hard materials, while those obtained by crosslinking in the molten state and following crystallization have softer properties.[14] These totally different properties can be made out and converted to each other simply by choosing thermal treatment. Molecular weight[15] and bonds connecting between prepolymers and terminal furan group[16] influence physical properties of both hard and soft properties. Though crystallization and crosslinking reaction proceed sequentially in the previous studies, coincidental development of crystals and crosslinks may give still other better properties to the network polymers.

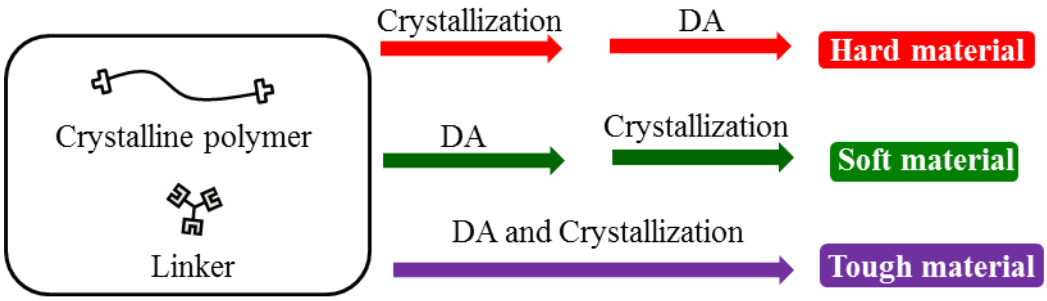

Figure 4-2. Mechanical property tuning of semicrystalline network polymers by controlling rates of crystallization and crosslinking

In this chapter, the author tried to further control the crystallization and crosslinking reaction during the preparation of the network polymers to obtain tough materials(Figure4-2).

Scheme1 (a) Chemical structures of $PCLF_2$, M_2 and M_3; (b) thermally reversible DA reaction of furan and maleimide

(a)

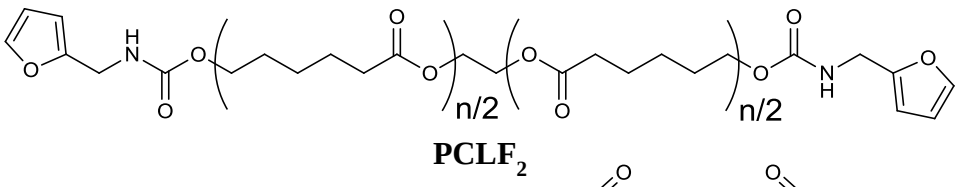

$PCLF_2$

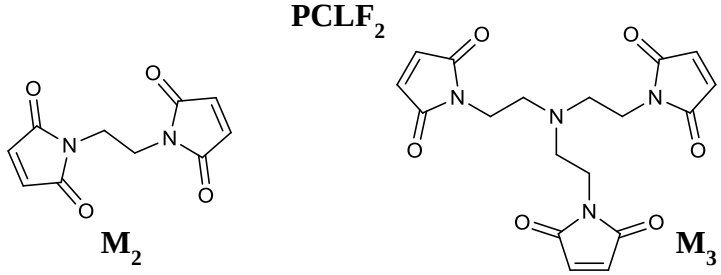

M_2 **M_3**

(b)

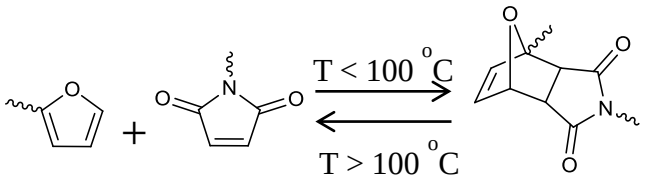

Furan **Maleimide** **DA adduct**

The author have chosen a furyl-telechelic poly(ε-caprolactone) ($PCLF_2$) and

tris(2-maleimide ethyl)amine (M_3) as a telechelic prepolymer and a linker, respectively (Scheme1).

First, crystallization rate of the $PCLF_2$ was analyzed by differential scanning calorimetry (DSC). Because of the difficulty to analyze insoluble network polymers, the DA reactivity was examined in the mixture of $PCLF_2$ and bis-maleimide (M_2) instead of the $PCLF_2/M_3$ mixture. Based on these results, network polymers from $PCLF_2$ and M_3 were prepared by various thermal conditions. Differences in properties of these network polymers were then investigated.

Experimental section

Materials.

All starting materials, reagents, and solvents were purchased from Tokyo Chemical Industry, Aldrich, Wako Pure Chemical Industries, Nacalai Tesque, or Kanto Chemical Co. and were used as received. M_2[17] and M_3[10] were synthesized as previously reported.

Synthesis of Prepolymer, [$PCLF_2$]

Ring opening polymerization of ε-caprolactone (20.0 g, 0.175 mol) was performed with ethylene glycol (0.300 ml, 4.86 mmol) as an initiator and $Sn(Oct)_2$ (0.079 g, 0.097 mmol) as a catalyst under a N_2 atmosphere at 120 °C for 24 h. Precipitation from chloroform into ice-cooled methanol gave PCL diol. ^{1}H NMR: M_n^{NMR} = 4400.

$PCLF_2$ was obtained by a terminal modification of PCL diol by a procedure described in our previous paper.[12] ^{1}H NMR: M_n^{NMR} = 5000. GPC: M_n^{GPC} = 8800, PDI = 1.12.

Synthesis of Network Polymers, $PCLF_2M_3$

Mixture of $PCLF_2$ and M_3 (molar ratio of furan/maleimide = 1/1.4) was prepared as a film cast from chloroform solution. The mixture were compression-molded between two Teflon sheets with an aluminum spacer (0.2 mm thickness) using a hot press (Imoto Co., Japan) at 145 or 150 °C for 30 min under a pressure of 6 MPa. Then the samples were quenched to a predetermined curing temperature, T_r, and kept for a predetermined time period, P_r, for crosslinking and crystallization. $PCLF_2M_3$(CRY), $PCLF_2M_3$(38), and $PCLF_2$M3(40) were prepared with T_r = room temperature, 38 °C and 40 °C and P_r = 6 days, respectively. $PCLF_2M_3$(44) and $PCLF_2M_3$(CL) were, respectively, prepared with T_r = 44 and 70 °C and P_t = 3 days, followed by keeping at room temperature for 1 day for crystallization.

DA Reaction between $PCLF_2$ and M_2

Progress of the DA reaction between furan and maleimide was traced in the mixture of $PCLF_2/M_2$ by ^{1}H NMR spectroscopy. Compression-molded films of the $PCLF_2/M_2$ mixtures (with molar ratio of furan/maleimide = 1/1.4) were prepared by a procedure similar to the $PCLF_2/M_3$ mixture described above. Then the samples were kept at 25, 38, 40, 44 and 70 °C and ^{1}H NMR spectra were measured at appropriate time intervals. Conversion to the DA adducts were calculated from the peak areas of the furan and DA adduct signals in the spectra.

Analytical Procedures.

^{1}H NMR spectroscopy was performed using a JEOL JNM-ECS400 NMR SYSTEM. Spectra were measured in chloroform-*d* at room temperature. Number-average molecular weight (M_n) and polydispersity index (PDI=M_w/M_n) were determined by gel permeation chromatography (GPC) on a Tosoh HLC-8220 GPC system equipped with two Tosoh TSK-GEL GMH_{HR}-N columns. Chloroform was used as an eluent with a flow rate of 1 mL min^{-1} at 40 °C. Polystyrene standards with low polydispersity were used to construct a calibration curve. Differential scanning calorimetry (DSC) was carried out on a Perkin Elmer Pyris 1 under a N_2 atmosphere. Samples in aluminum pans were measured. Melting point (T_m) and heat of fusion (ΔH_f) were taken as the peak top and area of melting endotherm during heating at a rate of 10 °C min^{-1}. Heat flow during isothermal crystallization was also observed at 25 °C, 38 °C, 40 °C and 44 °C. Samples were first thermally treated at 150 °C for 30 min and quenched to the crystallization temperature. Wide-angle X-ray diffraction (WAXD) measurement was performed on a Rigaku RINT-2000 diffractometer (40 kV and 40 mA) at room

temperature. Nickel-filtered Cu-Ka radiation (λ=0.154 nm) was used. WAXD patterns were analyzed by curve resolution into diffraction peaks from crystalline phase and an amorphous halo. The apparent crystallite size along the [*hkl*] direction (D_{hkl}) was determined using the Scherrer equation.[14,15,18] Tensile properties were evaluated using Shimadzu EZ test at a cross-head speed of 5 mm min^{-1} at room temperature.

Results and Discussion

Crystallization Rate of $PCLF_2/M_3$ Mixture at Various Temperature

Crystallization rate and equilibrium crystallinity of the $PCLF_2/M_3$ mixture at various temperatures were analyzed by DSC. During the preparation of the mixture, some DA adducts were generated from furan terminals of $PCLF_2$ and maleimide groups of M_3. In order to erase this reaction history, the sample was first thermally treated at 150 °C for 30 min, and then quenched to 25, 38, 40, or 44 °C. Heat flow was recorded at this temperature by DSC.

Table 4-1. Crystallization of $PCLF_2/M_3$ Mixtures at Various Temperatures

Crystallization Temperature	Isothermal Crystallization			Melting
	Peak top time[(a)] / min	Peak end time[(b)] / min	ΔH_c[(c)] / Jg^{-1}	ΔH_f / Jg^{-1}
25	0.17	0.58	37	58[(d)]
38	5.0	16	58	62[(d)]
40	12	54	65	61[(d)]
44	-[(e)]	-[(e)]	-[(e)]	1.3[(f)]

(a): Peak top time of exotherm during isothermal crystallization in DSC. (b):Peak end time of exotherm during isothermal crystallization. (c): Heat of crystallization during isothermal crystallization. (d): Heat of fusion during heating scans after the completion of the crystallization. (e): No exothermal peak was observed. (f): Heat of fusion during heating scans after isothermal crystallization for 1 hour.

The results are summarized in Table 4-1. When the mixture was kept at 25, 38 or 40 °C, an exothermal peak showing crystallization appeared on the DSC curve. At these

temperatures, crystallization ended in 0.58 min, 16 min and 54 min, respectively.

Though no peak appeared during isothermal crystallization at 44 °C, the heating scan following retention at 44 °C for 1 h had a small endothermal peak at 54 °C. This peak corresponds to the melting of PCL crystals, indicating that crystallization surely proceeded in the $PCLF_2/M_3$ mixture at 44 °C though the crystallization rate is very low. Therefore, at the temperature range between 25 and 44 °C, crystallization rate of PCL in the mixture decreases as the temperature increases.

DA Reaction between $PCLF_2$ and M_2 at Various Temperatures

All the $PCLF_2M_3$ samples were insoluble to chloroform, a good solvent for $PCLF_2$, indicating that three dimensional network structure is formed in $PCLF_2M_3$. Because of the difficulty to analyze the crosslinking reaction to generate insoluble network polymers, progress of the DA reaction was traced in the mixture of $PCLF_2$ and bis-maleimide, M_2, by ^1H NMR spectroscopy. The conversion to the DA adducts (including *exo* and *endo* forms) was calculated from the areas of the furan (7.33 ppm) and DA adduct signals (5.13-5.22 ppm) in the NMR spectra(Figure4-3(a)).

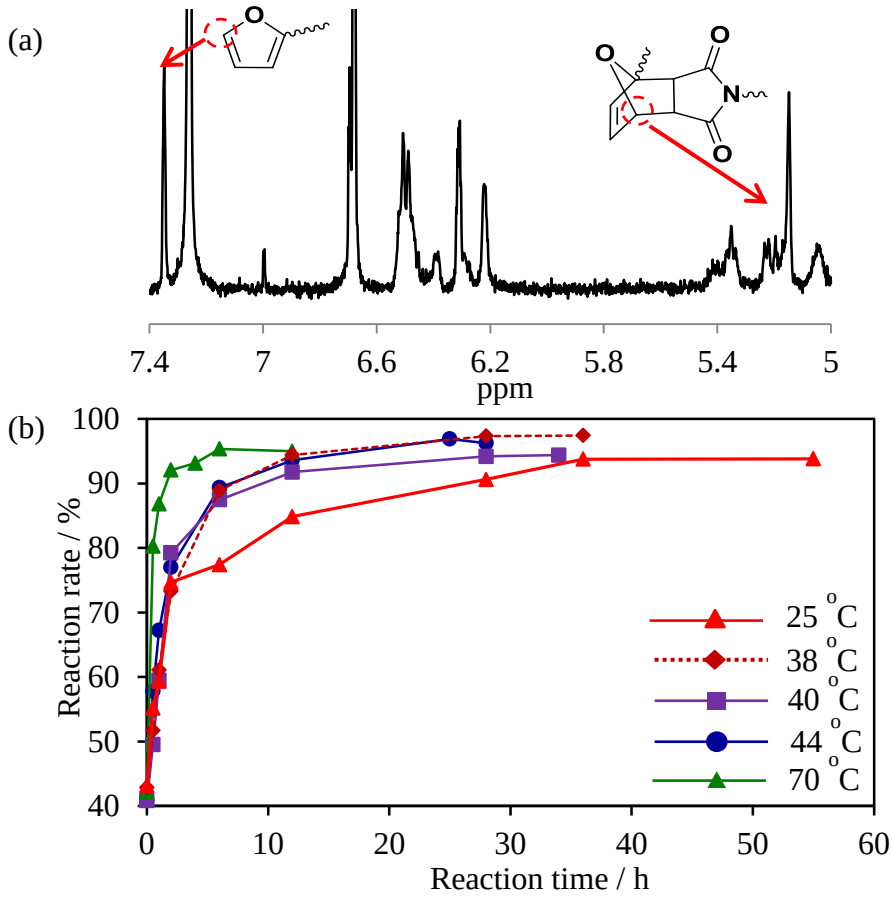

Figure 4-3. Progress of DA reactions in $PCLF_2/M_2$ determined by ^{1}H-NMR;(a) NMR spectrum of $PCLF_2/M_2$ in chloroform-d, (b) Reaction rate calculated from ^{1}H NMR spectra at various temperature

Table4-2 Rate of DA reactions

Temperature	Sample	Span of DA reaction / h	Conversion (1h) / %	Conversion (6h) / %	Equilibrium conversion / %
25	$PCLF_2+M_2$	36	59	77	95
38	$PCLF_2+M_2$	28	61	89	97
40	$PCLF_2+M_2$	28	60	87	94
44	$PCLF_2+M_2$	28	67	89	97
70	$PCLF_2+M_2$	12	89	95	94

The time courses of the conversion at temperatures between 25 and 70 °C are shown in Figure 4-3. At every temperature, the conversion exceeds 94% in the equilibrium. At 70 °C, the reaction reached equilibrium in 6 h, while it required 36 h at 25 °C. Between 38 and 44 °C, the reaction reached equilibrium in about 25 h.

The analysis of the DA reactivity was done with bis-maleimide linker (in $PCLF_2M_2$) while the crystallization analysis in the previous section was done with tris-maleimide linker (in $PCLF_2M_3$). The difference in the linker must surely influence the crystallization and reaction rates. However, as both of these analyses were done in the bulk sample without solvent, the influence must be not so significant.[14-16] The author can assume that the rate of the DA reaction in $PCLF_2/M_3$ is comparable to that in $PCLF_2/M_2$.

Sample Preparation of $PCLF_2$ and M_3 at Various Temperatures

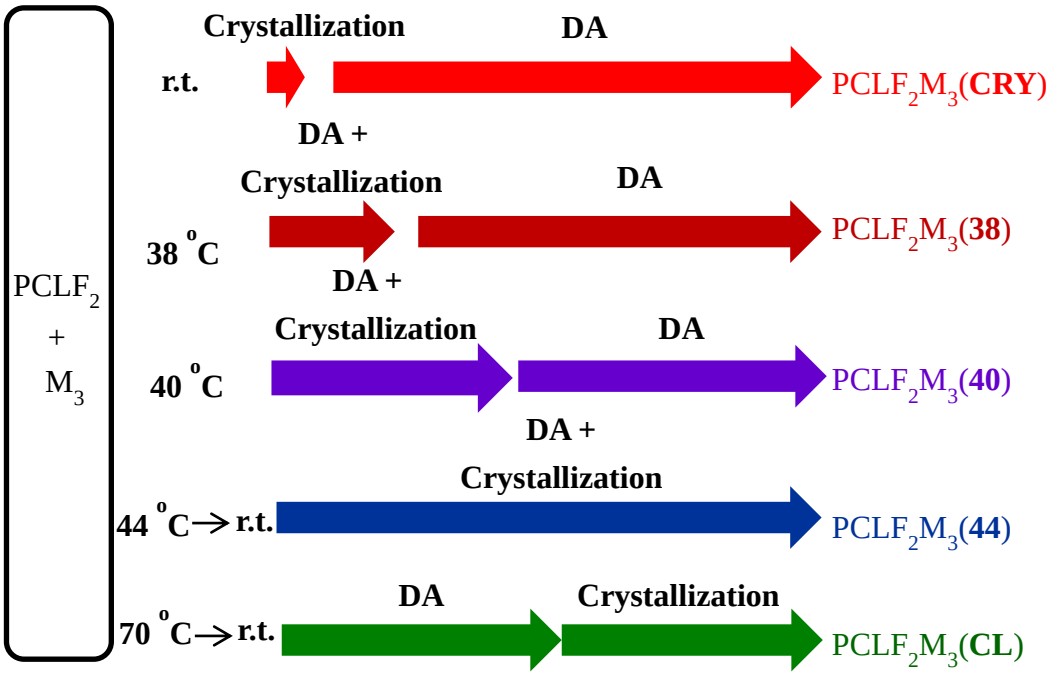

Figure 4-4. Sample preparation of $PCLF_2/M_2$ at various temperature

At room temperature, the crystallization (< 1min) is much faster than the DA reaction in $PCLF_2/M_3$. Therefore, in the preparation of $PCLF_2M_3$(CRY), the crystals are developed first, followed by crosslinking reaction. Since T_m of $PCLF_2$ is ≈ 55 °C, $PCLF_2M_3$(CL) is first crosslinked in the molten state followed by crystallization at room temperature. At 38, 40 and 44 °C , the DA reaction reaches equilibrium in about 25 h, while crystallization finishes in 16 min, 54 min and > 1 h, respectively. At the initial stage of the preparation of $PCLF_2M_3$(38), $PCLF_2M_3$(40), and $PCLF_2M_3$(44), crosslinking reaction competes with crystallization.

Thermal Properties of $PCLF_2M_3$ Prepared under Various Conditions.

Figure 4-5 shows DSC curves of $PCLF_2M_3$ during the heating scans.

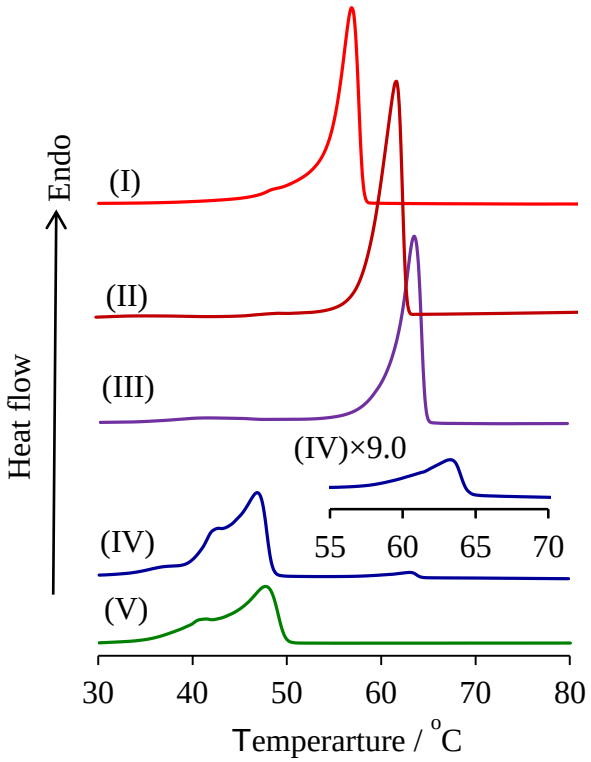

Figure4-5. DSC curves of (I)$PCLF_2M_3$(CRY), (II) $PCLF_2M_3$(38), (III) $PCLF_2M_3$(40), (IV) $PCLF_2M_3$(44), (V) $PCLF_2M_3$(CL). Inset is an enlarged view of (IV) around 65 °C

The T_m and ΔH_f values are listed in Table 4-3. Figure 4-5 and Table 4-3 show that T_m, ΔH_f and degree of crystallinity of $PCLF_2M_3$(CL) are lower than those of $PCLF_2M_3$(CRY). The preformed crosslinks in $PCLF_2M_3$(CL) restrict the crystallization and cause less ordered crystalline phase. T_m of $PCLF_2M_3$(38) and $PCLF_2M_3$(40) are yet higher than T_m of $PCLF_2M_3$(CRY). It happens usually in linear polymers that crystallization at higher temperature gives thermally more stable crystallites with a

Table 4-3. Thermal Properties and Crystallite Size of $PCLF_2M_3$.

Sample	T_m [a] / °C	ΔH_f [a] / Jg^{-1}	Degree of crystallinity [b] / %	D_{110} [c] / nm	D_{200} [c] / nm
$PCLF_2M_3$(CRY)	56	69	42	38	27
$PCLF_2M_3$(38)	61	64	39	40	45
$PCLF_2M_3$(40)	64	62	37	40	37
$PCLF_2M_3$(44)	47 / 63	46 / 2	29	27	23
$PCLF_2M_3$(CL)	48	48	29	32	25

(a): Determined by DSC. (b): Estimated by dividing ΔH_f of the sample by ΔH_f of 100 % crystalline $PCLF_2$ (166 Jg^{-1}). (c): Determined by WAXD.

higher melting point. Since the crystallization is completed in the very early stage of the crosslinking reaction in $PCLF_2M_3$(CRY), $PCLF_2M_3$(38) and $PCLF_2M_3$(40), influence of crosslinks to the crystallization is little. Therefore, T_m of them is in the order corresponding to the curing temperature. The ΔH_f values of $PCLF_2M_3$(38) and $PCLF_2M_3$(40) are a bit smaller than that of $PCLF_2M_3$(CRY) because of the slower crystallization, crosslinking.

The T_m and ΔH_f values are listed in Table 4-3. Figure 4-3 and Table 4-3 show that T_m, ΔH_f and degree of crystallinity of $PCLF_2M_3$(CL) are lower than those of $PCLF_2M_3$(CRY). The preformed crosslinks in $PCLF_2M_3$(CL) restrict the crystallization and cause less ordered crystalline phase. T_m of $PCLF_2M_3$(38) and $PCLF_2M_3$(40) are yet higher than T_m of $PCLF_2M_3$(CRY). It happens usually in linear polymers that crystallization at higher temperature gives thermally more stable crystallites with a higher melting point. Since the crystallization is completed in the very early stage of the crosslinking reaction in $PCLF_2M_3$(CRY), $PCLF_2M_3$(38) and $PCLF_2M_3$(40), influence of

crosslinks to the crystallization is little. Therefore, T_m of them is in the order corresponding to the curing temperature. The ΔH_f values of $PCLF_2M_3$(38) and $PCLF_2M_3$(40) are a bit smaller than that of $PCLF_2M_3$(CRY). Because of the slower crystallization, crosslinks in $PCLF_2M_3$(38) and $PCLF_2M_3$(40) might slightly affect the crystallization.

$PCLF_2M_3$(44) showed two-peak melting behavior (Fig. 4-5(IV)). A small endothermic peak is positioned at 63 °C with the main peak at 47 °C. Two melting peaks are often observed on the DSC melting curve of crystalline polymers. In such cases, multiple peaks arising from phase-separated crystals must be distinguished from those arising as a result of a melt/recrystallization during heating in a DSC apparatus. When DSC melting curves of $PCLF_2M_3$(44) recorded with different heating rates, 10, 15 and 20 °C min^{-1}, were compared (data not shown), the ratio of the peak areas at 47 and 63 °C were kept almost constant, showing the existence of the phase-separated crystals. The peak at 63 °C can be ascribed to the melting of the crystals formed in an early stage of isothermal crystallization at 44 °C, in which the crystallization is hardly disturbed by crosslinks. The peak top temperature, 47 °C, of the main peak is too close to the curing temperature, 44 °C. The crystal with such low T_m cannot be formed at 44 °C. This crystal must be formed at room temperature after curing at 44 °C. Actually, T_m at 47 °C corresponds to T_m of $PCLF_2M_3$(CL), in which crystals were developed at room temperature, while T_m at 63 °C is similar to T_m of $PCLF_2M_3$(38) and $PCLF_2M_3$(40).

WAXD analysis of $PCLF_2M_3$

Figure 4-6 displays WAXD patterns of $PCLF_2M_3$ samples.

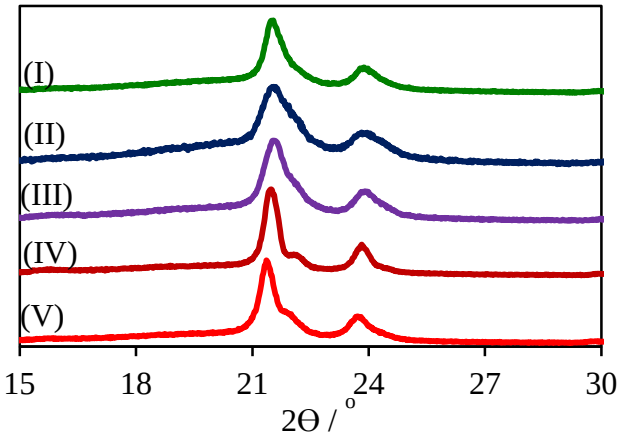

Figure 4-6. WAXD patterns of $PCLF_2M_3$ (I) $PCLF_2M_3$(CL), (II) $PCLF_2M_3$(44), (III) $PCLF_2M_3$(40), (IV) $PCLF_2M_3$(38), (V) $PCLF_2M_3$(CRY).

These patterns have three diffraction peaks at 2θ=21.5 °, 22.1 °, and 23.9 °, ascribable to the (110), (111) and (200) planes of the orthorhombic unit cell of PCL, respectively.[19] The peak width of the (*hkl*) diffraction is related to the mean crystallite size along the (*hkl*) direction, D_{hkl}, through the Scherrer equation.[18] From the peak width determined by curve resolution of the WAXD patterns, the D_{110} and D_{200} of $PCLF_2M_3$ were estimated (Table 4-4).

The crystallite size of $PCLF_2M_3$(CL) (D_{110} = 32 nm; D_{200} = 25 nm) is smaller than that of $PCLF_2M_3$(CRY) (D_{110} = 38 nm; D_{200} = 27 nm). These data indicate that relatively large crystallites can grow before network structure formation in $PCLF_2M_3$(CRY) while the preformed crosslinks in $PCLF_2M_3$(CL) disturb the development of large crystallites. The crystallites of $PCLF_2M_3$(38) and $PCLF_2M_3$(40) are rather larger than that of $PCLF_2M_3$(CRY). In $PCLF_2M_3$(38) and $PCLF_2M_3$(40), crystallization is also completed

in the very early stage of the crosslinking reaction. Therefore, larger crystallites are formed at higher temperature, as is usually happened to linear polymers. The crystallite size of $PCLF_2M_3(44)$ is obviously smaller than $PCLF_2M_3(38)$ and $PCLF_2M_3(40)$. As previously shown by the DSC analysis in this section, $PCLF_2M_3(44)$ has two crystalline phases. Smaller amount of large crystallites with T_m = 63 °C is formed at 44 °C while the following crystallization of larger amount of PCL at room temperature gives small crystallite (T_m = 47 °C) after crosslinking reaction. The D_{110} and D_{200} values apparently show the size of the latter crystalline phase. Therefore, the crystallite size of $PCLF_2M_3(44)$ is similar to that of $PCLF_2M_3(CL)$.

Network structures of $PCLF_2M_3$

By heating to 80 °C, the crystals in $PCLF_2M_3$ were melted without breaking the DA adducts. The crystallization in these melted samples (= 2nd crystallization) was analyzed by recording the heat flow during isothermal crystallization at room temperature and following heating on DSC.

Table 4-4. Second Crystallization[(a)] of $PCLF_2M_3$ at room temperature.

Sample	Peak top time[(b)] / min	Peak end time[(c)] / min
$PCLF_2M_3$ (CRY)	0.88	3.1
$PCLF_2M_3$ (38)	0.92	3.2
$PCLF_2M_3$ (40)	0.97	4.7
$PCLF_2M_3$ (44)	2.5	12
$PCLF_2M_3$ (CL)	5.1	14

(a): $PCLF_2M_3$ was melted at 80 °C without the dissociation of the DA adducts. Heat flow during the following isothermal crystallization was recorded at room temperature and analyzed. (b):Peak top time of exotherm during isothermal crystallization. (c):Peak end time of exotherm during isothermal crystallization.

The results are summarized in Table 4-4. The 2nd crystallization of $PCLF_2M_3$(CRY), $PCLF_2M_3$(38), $PCLF_2M_3$(40), $PCLF_2M_3$(44) and $PCLF_2M_3$(CL) finished in 3.1, 3.2, 4.7, 12, and 14 min, respectively. The difference in the 2nd crystallization rate relates with network structure and chain entanglements of $PCLF_2M_3$.[15] Higher rates of the 2nd crystallization in $PCLF_2M_3$(CRY), $PCLF_2M_3$(38) and $PCLF_2M_3$(40) indicate that these samples had fewer crosslinks in the network structure. As shown in Figure 4-3, the conversion of the DA reaction in the equilibrium is independent on the temperature. The

difference in the crosslink density in $PCLF_2M_3$ must be ascribed to the physical crosslinks by chain entanglements.

In the preparation of $PCLF_2M_3$(CRY), $PCLF_2M_3$(38) and $PCLF_2M_3$(40), the mixture of $PCLF_2$ and M_3 was kept at room temperature, 38 °C, or 40 °C, where relatively large crystals were developed first, followed by the DA reaction. This crystallization involves disentanglement and folding of linear $PCLF_2$. Therefore, the network structure with fewer entanglements was formed in these samples. On the other hand, in the preparation of $PCLF_2M_3$(CL) and $PCLF_2M_3$(44), the DA reaction preceded the crystallization. The chain entanglements in the mixture of $PCLF_2$ and M_3 were tied up by the DA reaction. Therefore, more apparent crosslinks, including chemical ones by DA adducts and physical ones by chain entanglements, were formed in $PCLF_2M_3$(CL) and $PCLF_2M_3$(44). This structural difference results in the difference in the 2nd crystallization rate. Among the former three samples, the 2nd crystallization rate of $PCLF_2M_3$(40) was a bit slower than $PCLF_2M_3$(CRY) and $PCLF_2M_3$(38), suggesting that crosslink density of $PCLF_2M_3$(40) was slightly higher.

Mechanical Properties of $PCLF_2M_3$ Prepared under Various Conditions.

Stress-strain curves of $PCLF_2M_3$ samples are shown in Figure 4-7.

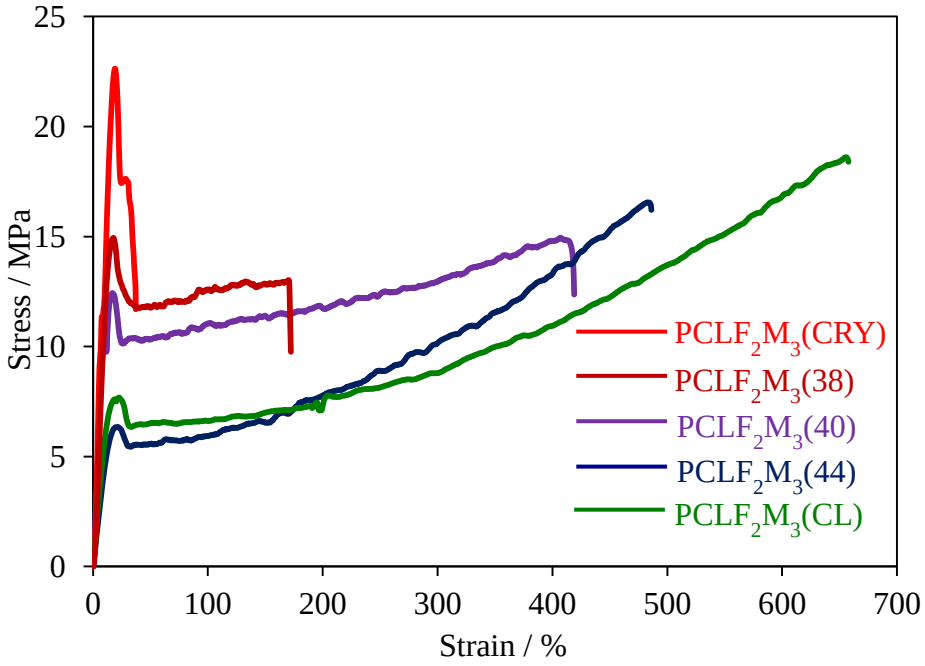

Figure 4-7. Stress-strain curves of $PCLF_2M_3$

Table 4-5. Tensile Properties of $PCLF_2M_3$

Sample	Stress at yield / MPa	Young modulus / MPa	Elongation at break / %
$PCLF_2M_3$(CRY)	22 ± 1	184 ± 23	47 ± 8
$PCLF_2M_3$(38)	14 ± 0.6	137 ± 31	187 ± 98
$PCLF_2M_3$(40)	12 ± 1	139 ± 5	458 ± 70
$PCLF_2M_3$(44)	7 ± 0.2	53 ± 12	494 ± 56
$PCLF_2M_3$(CL)	7 ± 1	71 ± 6	641 ± 79

Young modulus, stress at yield and elongation at break of the samples are listed in Table 4-5. $PCLF_2M_3$(CRY) was a hard material with high Young modulus, high and

clear yield point and small elongation at break, while $PCLF_2M_3$(CL) was a soft and ductile material with large elongation at break. The mechanical properties of $PCLF_2M_3$(38), $PCLF_2M_3$(40) and $PCLF_2M_3$(44) are positioned between $PCLF_2M_3$(CRY) and $PCLF_2M_3$(CL). As the preparation temperature is increased from room temperature (CRY) through 38, 40 °C, and 44 °C to 70 °C (CL), stress at yield and Young modulus are decreased while elongation at break is increased. These mechanical characteristics must come from difference in the structural parameters. Stress at yield and Young modulus depends on the crystal sizes and the degree of crystallinity: samples with larger crystal and higher crystallinity have higher stress at yield and Young modulus. Elongation at break depends on network structures: samples with higher apparent (chemical + physical) crosslink density are more stretchable.

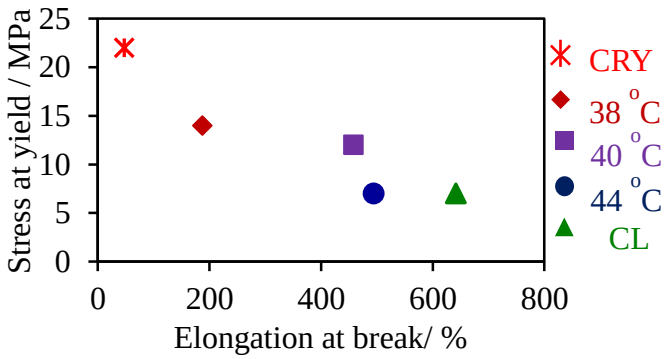

Figure4-8 Relation between stress at yield and elongation at break of $PCLF_2M_3$

Based on the structural characteristics, the $PCLF_2M_3$ samples were easily categorized into two groups. One includes $PCLF_2M_3$(CRY), $PCLF_2M_3$(38) and $PCLF_2M_3$(40) in which crystallization were proceeded before the DA reaction, and the other includes $PCLF_2M_3$(44) and $PCLF_2M_3$(CL), in which formation of the DA adducts was followed by crystallization. Figure 4-8 shows the relation between stress at yield and elongation

at break of $PCLF_2M_3$. Interestingly, mechanical properties of the samples cannot be classified into two groups. Their properties change rather continuously and no clear boundary is found between these groups. In the preparation of $PCLF_2M_3$(38), $PCLF_2M_3$(40) and $PCLF_2M_3$(44), crystallization and crosslinking must disturb the development of each other to give complex structure with moderate crosslink density and moderate crystallinity, which results in tough and ductile materials.

Additionally, mechanical properties of $PCLF_2M_3$ can be changed by molecular weight of $PCLF_2$. Table 4-6 shows that mechanical properties of $PCLF_2M_3$, which were constructed from two kinds of $PCLF_2$. These were different in molecular weight(M_n^{NMR} = 5000 and 5400). $PCLF_2M_3$(CRY), $PCLF_2M_3$(CL), and $PCLF_2M_3$(40) were prepared from both $PCLF_2$.

Table 4-6. Tensile Properties of $PCLF_2M_3$ consisting of two kinds of $PCLF_2$

Sample	M_n^{NMR} of $PCLF_2$			
	5000		5400	
	Stress at yield / MPa	Elongation at break / %	Stress at yield / MPa	Elongation at break / %
$PCLF_2M_3$(CRY)	22 ± 1	47 ± 8	25 ± 0.6	17 ± 1
$PCLF_2M_3$(40)	12 ± 1	458 ± 70	17 ± 2	393 ± 30
$PCLF_2M_3$(CL)	7 ± 1	641 ± 79	12 ± 0.8	486 ± 63

In comparison to $PCLF_2M_3$ with lower molecular weight $PCLF_2$, $PCLF_2M_3$_5400 consisting of $PCLF_2$ with higher M_n^{NMR} had higher stress at yield and lower elongation at break, shown in Figure4-9.

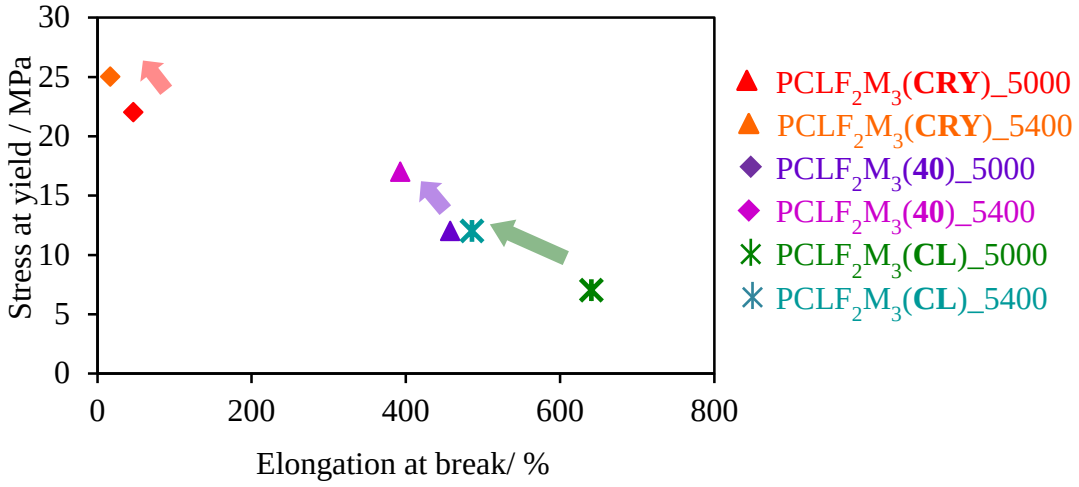

Figure4-9 Relation between stress at yield and elongation at break of $PCLF_2M_3$ consisting of two kinds of $PCLF_2$

These results indicate that molecular weight of PCLF2 affects mechanical properties of $PCLF_2M_3$.

On the other hand, $PCLF_2M_3$ can be converted to the other $PCLF_2M_3$ by melting or rDA reactions. In the previous research, crystalline network polymers after melting without dissociation of crosslinks and following crystallization at room temperature became softer than original because of presence of network structure.[14,15] $PCLF_2M_3$(40) was melted at 80 °C and crystalized to obtain $PCLF_2M_3$(40-80-CL).

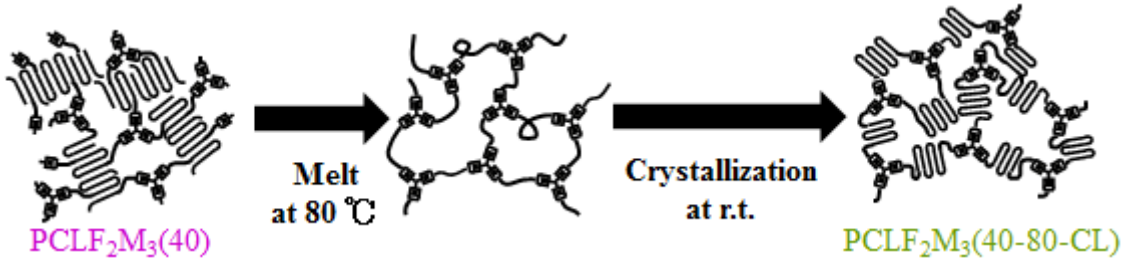

Figure4-10 Conversion of $PCLF_2M_3$(40) to $PCLF_2M_3$(40-80-CL) by melting

Mechanical properties of $PCLF_2M_3$(40-80-CL) were similar to those of $PCLF_2M_3$(CL), shown in Figure4-11 and Table 4-7. Properties of obtained polymers after melting and following crystallization depend on network structures of original polymers. Table 4-4 showed that the network of $PCLF_2M_3$(40) had a little chain entanglements, therefore $PCLF_2M_3$(40-80-CL) resemble $PCLF_2M_3$(CL).

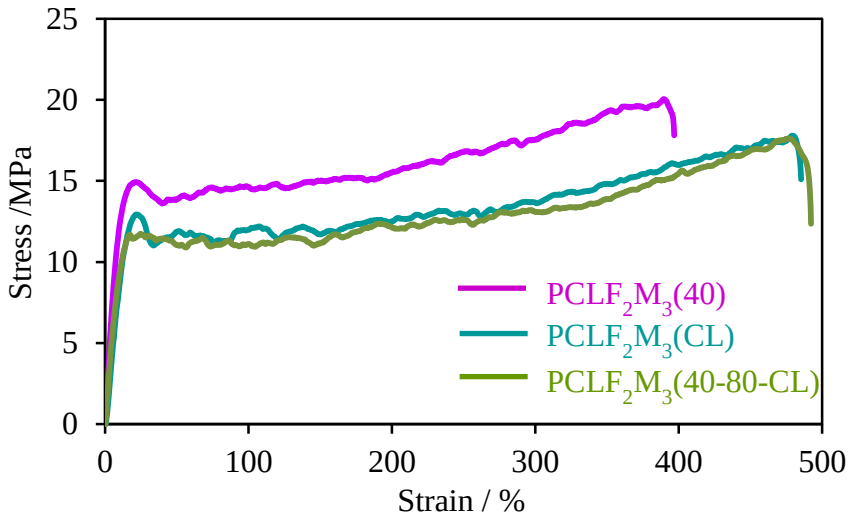

Figure4-11 Stress-strain curves of $PCLF_2M_3$(40), $PCLF_2M_3$(CL), and $PCLF_2M_3$(40-80-CL)

Table 4-7. Tensile Properties of $PCLF_2M_3$(40), $PCLF_2M_3$(CL) and $PCLF_2M_3$(40-80-CL)

Sample	Stress at yield / MPa	Young modulus / MPa	Elongation at break / %
$PCLF_2M_3$(40)	17 ± 2	146 ± 27	393 ± 30
$PCLF_2M_3$(40-80-CL)	13 ± 1	109 ± 14	529 ± 49
$PCLF_2M_3$(CL)	12 ± 0.8	88 ± 18	486 ± 63

Network polymers in this research consists of PCL crosslinked by DA adducts, therefore $PCLF_2M_3$ can be reinstated to $PCLF_2$ and M_3 by rDA and they can be re-constructed to the other $PCLF_2M_3$ by crystallization and crosslinking at appropriate temperatures.

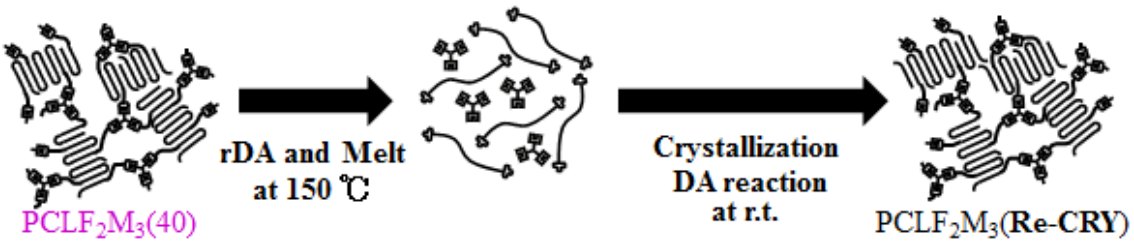

Figure4-12 Conversion of $PCLF_2M_3$(40) to $PCLF_2M_3$(Re-CRY) by rDA

$PCLF_2M_3$(Re-CRY) was prepared from $PCLF_2M_3$(40) by rDA and following immediate crystallization and gradual DA reactions at room temperature. In compared to $PCLF_2M_3$(CRY), mechanical properties of $PCLF_2M_3$(Re-CRY) were almost the same, shown in Figure4-13 and Table4-8. These results $PCLF_2M_3$ can be converted to the other $PCLF_2M_3$ by rDA and following crystallization and crosslinking.

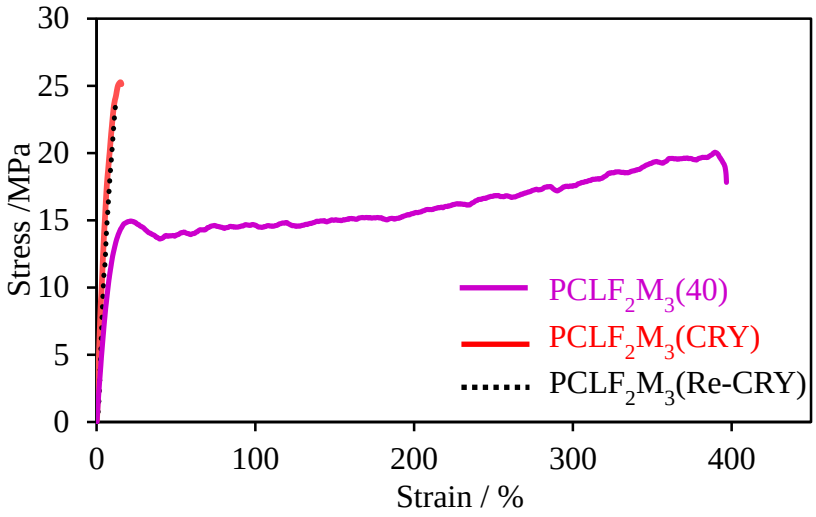

Figure4-13 Stress-strain curves of $PCLF_2M_3(40)$, $PCLF_2M_3(CRY)$ and $PCLF_2M_3(Re\text{-}CRY)$

Table 4-8. Tensile Properties of $PCLF_2M_3(40)$, $PCLF_2M_3(CL)$ and $PCLF_2M_3(Re\text{-}CRY)$

Sample	Stress at yield / MPa	Young modulus / MPa	Elongation at break / %
$PCLF_2M_3(40)$	17 ± 2	146 ± 27	393 ± 30
$PCLF_2M_3(CRY)$	25 ± 0.6	351 ± 60	17 ± 1
$PCLF_2M_3(Re\text{-}CRY)$	24 ± 3	347 ± 69	13 ± 2

Conclusion

In this study, the author has tuned mechanical properties of network polymers prepared by DA reaction of a furyl-telechelic crystalline prepolymer $PCLF_2$ and a tris-maleimide linker M_3. The rate of two dynamic processes, i.e., crosslinking reaction and crystallization are controllable by changing the curing temperature. When the $PCLF_2/M_3$ mixture was cured at a temperature much below T_m of PCL, crystallization proceeded first, followed by crosslinking reaction. Curing above T_m promoted the precedent crosslinking, which is followed by the crystallization at room temperature. The former curing gave a hard and stiff material, while the latter gave a soft and stretchable one. Curing between these temperatures allowed coincidental development of crystals and crosslinks., which gave tough and ductile materials. The structural analysis of the network polymers prepared at various curing conditions showed that the variation in the mechanical properties were ascribable to the difference in crystallinity, crystallite size and crosslink density, which came from the sequencing of crystallization and DA reactions. Therefore, materials with various mechanical properties, from soft to hard, can be obtained by simply controlling the curing temperature and time. Additionally, decrosslinking reaction of $PCLF_2M_3$ proceeds above 100 °C. The resultant $PCLF_2$ and M_3 can be recrosslinked to $PCLF_2M_3$ with different mechanical properties. Thus, $PCLF_2M_3$ is a switchable and recyclable material.

Reference

[1](a) E. Sato,; H. Tamura, A. Matsumoto, *ACS Appl. Mater. Interfaces*, **2010**, *2*, 2594, (b) R. Wang, X. Xiao, T. Xie, *Macromol.. Rapid Commun*. **2010**, *31*, 295.

[2](a)Y. Okumura, K. Ito, *Adv. Mater*. **2001**, *13*, 485-487., (b)J. P. Gong, Y. Katsuyama, T. Kurokawa, Y. Osada, Adv. Mater. **2003**, *15*, 1155.

[3] (a)Y. Amamoto, J. Kamada, H. Otsuka, A. Takahara, K. Matyjaszewski, *Angew. Chem. Int. Ed.* **2011**, *50*, 1660., (b)E.D. Rodriguez, X. Luo, T. Patrick, P.T. Mather, *ACS Appl. Mater. Interfaces*, **2011**, *3*, 152.

[4] (a)G. Zhu, G. Liang, Q. Xu, Q.Yu, *Journal of Applied Polymer Science*, **2003**, *90*, 1589., (b)E. Delrio, G. Lligadas. J.C. Ronda, M. Galia, M. A. R. Meire, V. Cadiz, *J Polym Sci Part A: Polym Chem*, **2011**, *49*, 518.

[5] A. J. Peacock, *J. Macromol. Sci., Polym. Rev.* **2001**, *C41*, 285.

[6] I. Chod_ak, *Prog. Polym. Sci.* **1998**, *23*, 1409–1442.

[7] (a) L. Zheng, A. J. Waddon, R. J. Farris, E. B. Coughlin, *Macromolecules* **2002,** *35*, 2375, (b) H. Kang, Q. Lin, R. S. Armentrout, T. E. Long, *Macromolecules* **2002**, *35*, 8738.

[8] R. J. Wojtecki, M. A. Meador, S. J. Rowan, *Nature materials*, **2011,** *10*, 14.

[9] (a) Y. Imai, H. Itoh, K. Naka, Y. Chujo, *Macromolecules*, **2000,** *33*, 4343, (b) A. A. Kavitha, N. K. Singha, *Macromolecules* **2010**, *43*, 3193, (c) T. Defize, R. Riva, J. M. Raquez, P. Dubois, C. Jerome, M. Alexandre, *Macromol Rapid Commun.* **2011**, *32*, 1264.

[10] X. X. Chen, M. A. Dam, K. Ono, A. Mal, H. B. Shen, S. R. Nutt, K. Sheran, F. Wudl, *Science*, **2002**, *295*, 1698.

[11] M. Watanabe, N.Yoshie, *Polymer* **2006**, *47*, 4946.

[12] K. Ishida, N. Yoshie, *Macromol Biosci* **2008**, *8*, 916.

[13] N. Yoshie, M. Watanabe, H. Araki, K. Ishida, *Polym. Degrad. Stab.*, **2010**, *95*, 826.

[14] K. Ishida, N. Yoshie, *Macromolecules* **2008**, *41*, 4753.

[15] K. Ishida, Y. Nishiyama, Y. Michimura, N. Oya, N. Yoshie, *Macromolecules* **2010**, *43*, 1011.

[16] K. Ishida, V. Weibel, N. Yoshie, *Polymer* **2011**, *52*, 2877.

[17] A. A. Kumar, K. Dinakaran, M. Alagar,. *J. Appl. Polym. Sci.* **2003**, *89*, 3808.

[18]L. E. Alexander LE. *X-ray diffraction Methods in polymer Science*. New York: Wiley-Interscience, **1969.**

[19] **S.** Nojima, K. Hashizume, A. Rohadi, S. Sasaki, *Polymer* **1997**, *38*, 2711.

Chapter 5.

Conclusion

Conclusion

In this study, the author obtained three kinds of functional materials. These materials with novel functions were obtained from crystalline polymers with dynamic bonds by controlling crystallization and formation of dynamic bonds.

In Chapter 2, the author descried on a photoinduced mendable network polymer. The polymer crosslinked by cinnamate dimers were obtained by photoirradiation and heating of cinnamoyl-telechelic poly(butylene adipate) ($PBAC_2$) and pentaerythritol tetracinnamate (C_4). Although *trans-cis* isomerization and dimerization of the cinnamoyl groups proceeded together by photoirradiation, heating promoted dimerization more to form a network polymer. This cinnamate polymer had a photoinduced mending ability. Damage to this network polymer induced breaking of cynnamate dimers to form cinnamate monomers. This broken network could be mended by photoirradiation which was led by re-dimerization of cinnamate monomers at damaged surfaces.

In Chapter 3, the author described on crystalline polymers with mending ability at room temperature. The author proposed a novel approach to obtain mendable crystalline polymers at room temperature. To achieve this purpose, crystalline polymers were end-functionalized with bulky tolylene and hydrogen bonding ureidopyrimidinone (UPy) units to reduce crystallization rate. Poly(ethylene adipate) end-functionalized with tolylene and UPy units(PEA-toly-UPy) were combined by hydrogen bonds to construct a supramolecular polymer. Cutting of PEA-toly-UPy samples invokes dissociation of hydrogen bonds and reduction of crystallinity at the cut surfaces. Compared with the faster crystallizing polymer, UPy-hexyl-telechelic PEA, higher molecular mobility at the cut surfaces of PEA-toly-UPy was maintained for a longer

period due to the slow crystallization, which allowed the reformation of dynamic bonds between the cut surfaces to repair. Because of the reversibility of the dynamic bond, this mending mechanism worked repeatedly at the same position.

Additionally, improvement of mechanical properties of PEA-toly-UPy was described. Crystalline polymer, poly(ethylene succinate)(PES), was inserted into the center of PEA-toly-UPy to form ABA type block polymer. This ABA block polymer, PEA-PES-UPy, had more elasticity because PES segments with crystallization and phase separation acted as physical cross-linking points. PEA-PES-UPy also had repeatable mending ability at room temperature.

In Chapter 4, the author descried on mechanical property tuning of semicrystalline network polymers by controlling rates of crystallization and crosslinking. Network polymers were obtained from furyl-telechelic poly(ε-caprolactone) ($PCLF_2$) and a tris-maleimide linker (M_3) by Diels-Alder reactions. Cross-linking by DA reactions and crystallization can be control by preparation temperature. When the polymer was prepared at room temperature, a hard material was obtained by immediate crystallization and following cross-linking by DA reactions. The polymer cross-linked above melting points and crystallized at room temperature gave a soft material. When the polymer was prepared at around 40 ^{o}C, crystallization and crosslinking progressed at the same time, which leads to hard materials. Crosslinking and crystallization did not disturb each other for short periods from start. Therefore, crystalline and network structures became different from the other materials. By controlling rate of crystallization and cross-linking, tuning of mechanical properties of semicrystalline network polymers became possible with soft, tough and hard properties.

In the previous research of crystalline polymers with dynamic bonds, crystallization or formation of dynamic bond progressed under the condition where the other did not occur. The material in Chapter 2 is prepared under this condition. Network did not form at room temperature because low molecular mobility inhibited cinnamate dimerization. Crosslinks by cinnamate dimers formed under molten condition, resulting in the mendable network polymer. Like this research, crystals sometimes interfere with formation of dynamic bonds. Therefore, keeping above melting points, which disturb crystallization, and following crystallization is one of the most effective methods to fabricate materials and make materials fulfill their functions.

In Chapter3, heating of whole samples above melting points was not necessary for exhibition of materials' functions, mending ability. Materials with dynamic bonds have possibility to mend because weak dynamic bonds may preferentially break by damage. Material will mend, if they reform. However, most of materials with dynamic bonds do not mend at room temperature because crystals reduces molecular mobility. If materials are heated above melting points, dynamic bonds can reform to mend. Controlling rates of crystallization by polymer structures makes the reformation of dynamic bonds between damaged surfaces possible because higher molecular mobility is maintained. Therefore, crystalline polymers with dynamic bonds can exhibit their innate functions at room temperature. Like this research, controlling rate of crystallization, which leads to reformation of dynamic bonds, can make materials exhibit novel functions other than mending ability.

Additionally, progress of crystallization and formation of dynamic bonds give materials with new properties, as shown in Chapter4. This control performed by temperature has never been considered in previous research: Most of the materials were

prepared by making dynamic bonds first followed by crystallization because formation of dynamic bonds took priority. This tuning of mechanical properties is worth due to fulfilling the requests of applications.

In these studies, the author used poly(buthylene adipate), poly (ethylene adipate), poly(ethylene succinate), and poly(ε-caprolactone) as crystalline polymers. Additionally, cinnamoyl dimers, hydrogen bonds, and Diels-Alder adducts were chosen as dynamic bonds. These resulted in materials with different properties and functions. When materials consisting of crystalline polymers and dynamic bonds were fabricated, properties and functions depend on the main chain of crystalline polymer and the dynamic bonds. However, these choices are not dominate. Controlling crystallization and dynamic bonds give new functions. Additionally, their control expands the capacity of crystalline polymers with dynamic bonds. Other crystalline polymers with other dynamic bonds have possibilities of having mendability at room temperature by controlling rate of crystalline because this function comes from reformation of dynamic and slow crystallization. Mechanical property tunning can be also performed to other combination.

In conclusion, the author reveals through this doctoral research that controlling the rate of crystallization and formation of dynamic bonds can expand the potential of crystalline polymers with dynamic bonds and become new methods which generate novel functional materials.

Publication list

Nobuhiro Oya, Petty Sukarsaatmadja, Kazuki Ishida, Naoko Yoshie

Photoinduced mendable materials from poly(butylene adipate) end-functionalized with cinnamoyl groups

Polymer journal accepted

Nobuhiro Oya and Naoko Yoshie

A crystalline polymer with a self-mending ability at room temperature

In preparation.

Nobuhiro Oya, Shunsuke Saitoh, Yukiko Huruhashi and Naoko Yoshie

Mechanical property tuning of semicrystalline network polymers by controlling rates of crystallization and crosslinking

Journal of Polymer Science Part A: Polymer Chemistry accepted

Acknowledgment

During doctoral dissertation, the author deeply indebted to many people for advice and support. The author would like to thank them all, but mentioning only a few is allowed here.

First, the author would like to express my profound gratitude to his supervisor, Professor Naoko Yoshie, for her significant discussion, continued advices, and invaluable guidance throughout the work.

The author is deeply grateful to the member of this thesis committee, Professor Kenichi Hatanaka, Professor Tetsu Tatsuma, Professor Takeshi Serizawa and Associate Professor Hirohiko Houjou for their valuable and helpful advices for summarizing this work.

The author wishes to greatly acknowledge Postdoctoral Research Associate Kazuki Ishida for his technical advice and experimental guidance. The author wishes to express his gratitude to Assistant Professor Hidetake Seino for his helpful discussion and hearty encouragement.

The author would like to acknowledge Associate Professor Masaru Ogura for TG and XRD analysis. The author wishes to express his gratitude Professor Koji Araki and Technical Support Specialist Isao Yoshikawa for DSC analysis.

The author wishes to gratefully acknowledge the members of Yoshie laboratory, Dr. Hirotaka Ejima, Ms. Hitomi Araki, Mr Tomohiko Hasegawa, Ms. Petty Sukarsaatmadja, Ms. Akane Watanabe, Mr. Ryota Hasuno, Mr. Junya Shimazaki, Ms. Violaine Weibel, Mr. Akira Matustani, Mr. Shunsuke Saito, Mr. Shunsuke Kodama, Mr. Alexis Macala, Mr. Takehiro Fujita, Mr. Tabito Ikezaki, Mr. Naohiro Ueda, Mr. Kazuhiro Ogita, Ms Satsuki Shinohara, Mr. Zhang Xin, Mr. Zeng Chao, for their helpful discussion and

cordial encouragements. The author belonged Yoshie laboratory for 5 years. It was five invaluable years for him.

This research was supported in part by the Global COE Program for Chemistry Innovation through Cooperation of Science and Engineering from the Ministry of Education, Culture, Sports, Science and Technology (MEXT), Japan.

Finally, the author acknowledges my parents for their constant support and encouragement.

Department of Chemistry and Biotechnology

Graduate School of Engineering

Institute of Industrial Science

The University of Tokyo

Nobuhiro Oya